Comparative study of Chronic Ulcerative Dermatopathy in cultured meagre, *Argyrosomus regius*.

Tsertou M.I.[a,b], Papandroulakis N.[b], Keklikoglou K.[b,c], Kalantzi I.[d], Tsapakis M.[d], Tsalafouta A.[d], Pavlidis M.[d] Antonopoulou E.[a], Katharios P.[b*]

[a] Laboratory of Animal Physiology, Department of Zoology, School of Biology, Faculty of Sciences, Aristotle University of Thessaloniki, 54124 Thessaloniki, Greece

[b] Institute of Marine Biology, Biotechnology and Aquaculture, Hellenic Centre for Marine Research, Former American Base of Gournes, Heraklion 71003, Crete, Greece

[c] Biology Department, University of Crete, 70013 Heraklion, Crete, Greece

[d] Laboratory of Fish Physiology, Department of Biology, University of Crete, Heraklion, Greece

[e] Institute of Oceanography, Hellenic Centre for Marine Research, Former American Base of Gournes, Heraklion 71003 Heraklion, Crete, Greece

[*] Corresponding author. Email address: katharios@hcmr.gr

Abstract

Chronic Ulcerative Dermatopathy (CUD) is a disease that affects all cultured meagre when reared in facilities supplied with borehole water, resulting in ulceration of the skin overlying the lateral line canals. The aims of this study were (i) to describe the morphogenesis of the cephalic lateral line, (ii) to investigate the effect of the use of borehole water vs natural seawater in the development of the disease, (iii) to assess the recovery of the lesions and (iv) to evaluate the effect of CO_2 and pH on the development of CUD. The development of the lateral line canals in the head was completed by day 28 post hatching when fish were 19.3 mm in total length, while the source of the water did not affect the developmental process. The characteristic lesions of CUD were induced when meagre were reared in borehole water, while the lesions were resolved when fish were transferred to natural seawater. Lesions were

macroscopically visible by day 56 post hatching. Moreover, significant differences in the expression of genes regulating osteoclast's activity were observed between healthy and CUD-affected fish, while neither pH nor CO_2 were involved in the development of the disease. Finally, higher concentrations of heavy metals were found in the heads of CUD-affected meagres reared in borehole water compared to healthy fish reared in natural seawater.

Keywords: lateral line, erosion, ulcer, micro-CT, histopathology, heavy metals, water quality, meagre

1. Introduction

The lateral line is a mechanosensory system found in all fishes and in the larvae of aquatic amphibians, which is used for the detection of water movements and/or pressure fluctuations (Bleckmann and Zelick, 2009; Mogdans et al., 2004). The receptors of the lateral line that detect water flow are called neuromasts and they are distributed on the head, the trunk and the tail of the fish. Neuromasts can be either superficial on the skin or enclosed in the fluid-filled canals of the lateral line that open to the environment through a series of pores (Bleckmann and Zelick, 2009; Webb, 1989). The development and maintenance of the lateral line canals is achieved through a bone remodeling process which includes the participation of both osteoclasts (bone-resorption cells) and osteoblasts (bone-forming cells) (Wada et al., 2014; Webb, 2013).

Several conditions affecting the lateral line organ of the head and the trunk of various marine and freshwater fish have been reported under the terms, hole-in-the-head, Head and Lateral Line Erosion syndrome (HLLE) and Lateral Line Depigmentation (LLD) (Corrales et al., 2009; Morrison et al., 2007; Noga, 2010). Apart from these, Chronic Ulcerative Dermatopathy (CUD) is a pathological condition affecting the lateral line canals of freshwater and marine cultured fish species. It was first described in the Australian freshwater fish Murray cod (*Maccullochella peelii peelii* (Mitchell)), when reared in sites supplied by groundwater (Baily et al., 2005; Ingram et al., 2004; Schultz et al., 2011, 2008). The clinical signs of this first report included focal erosion, ulceration and loss of epidermis around the lateral line

canals of the head and the trunk and fin erosion. It has been associated with reduced growth rates, increased mortalities and significant reduction of marketability due to the severe disfigurement of the affected fish (Baily et al., 2005; Ingram et al., 2004; Schultz et al., 2008). Due to the localization of the lesions exclusively on the lateral line canals, it was hypothesized that the disease mechanism involved the binding of an unknown waterborne toxin to the mucus content of the sensory canals, resulting in focal hyperplasia and necrosis. Moreover, it was shown that when CUD-affected Murray cod were transferred to river water, the majority of the fish were structurally recovered after a period of 8-10 weeks. Based on these results and in the absence of viral or bacterial agents, it was suggested that some component of the groundwater was the driving force for the development of CUD. However, after analysis of basic water quality parameters as well as heavy metal and pesticide/insecticide content of the groundwater, the exact component of the water that could have resulted in the development of the disease could not be identified. Following the association of groundwater with the disease, several water treatment methods were evaluated in order to reduce the severity of the lesions on Murray cod, including electrolyte enrichment, pre-treatment with UV irradiation and pre-conditioning of groundwater either in a vegetated earthen pond or in tanks containing artificial macrophytes (Schultz et al., 2011). Amongst them, pre-conditioning of the water for 72h into a vegetated earthen pond or a tank containing biofilms growing on an artificial macrophyte, was found to be an effective method for the reduction of both the incidence and the severity of CUD in juvenile Murray cod (Schultz et al., 2011)

Regarding marine fish species, CUD was described in sharpsnout seabream (*Diplodus puntazzo)* when cultured in saline borehole water (Katharios et al., 2011). The CUD-affected fish exhibited bilateral lesions in the head canals of the lateral line and eroded fins and recovery of the lesions was also observed following transfer of the fish to natural sea water. By excluding an infectious agent for the onset of the disease and in an attempt to determine the causative agent of CUD in sharpsnout seabream it was hypothesized that borehole water, which was rich in CO_2, as indicated also by the lower pH compared to the pH of natural seawater, increases the enzymatic activity of the osteoclasts (Katharios et al., 2011). In this scenario, there would be an environmentally induced imbalance between osteoclasts and osteoblasts

that would cause the lesions seen in the fish, located exclusively in the lateral line canals which are in direct contact with the water.

A range of marine fishes have been reported as CUD-sensitive including one of the most important marine aquaculture species, European seabass (*Dicentrachus labrax*). The lesions in the seabass become visible when the fish is more than 5g. Although most of the hatcheries in the Mediterranean use borehole water, the disease was undetected until recently due to the common practice of growing the fish in inland facilities until 2-3g and then transfer it to sea cages. Many hatcheries changed their strategy and grew the seabass in larger size before the transportation to sea cages so the disease became apparent and a bigger concern for the producers since the damaged epidermis could affect the susceptibility of the fish to a wide range of pathogens in the sea (Katharios, personal observations).

Apart from the seabass and sharpsnout seabream, meagre (*Argyrosomus regius*) which is an emerging species for the Mediterranean aquaculture was found also to be sensitive to CUD when reared in facilities supplied with borehole water. The disease affects 100% of the population and results in ulceration of the skin overlying the lateral line canals, however, it is not associated with mortalities (Rigos and Katharios, 2010; Soares et al., 2018). The aim of this study is to describe the morphogenesis of the lateral line organ in the head of meagre as it is the organ affected from CUD and to describe the disease using histology, scanning electron microscopy (SEM) and microcomputed tomography (μ-CT). In addition, the osteoclast activity was investigated in CUD-affected fish using molecular markers while the CO_2 in the water was examined as the aetiological factor of the disease.

2. Materials and Methods

2.1 Ethics

All animal experimental procedures and handling in this study were conducted in the HCMR's licensed facility (EL91-BIOexp-04) under the protocol 255332 (29/11/2017) approved by the regional veterinary authority, which is the competent agency according to the Directive 2010/63/EU.

2.2 Rearing trial for the description of the disease

Two parallel rearing trials of meagre in borehole and natural seawater, respectively, were conducted in order to study the development of CUD. The eggs used in this study were obtained from a broodstock maintained at the facilities of the Institute of Marine Biology, Biotechnology and Aquaculture, HCMR, Crete, Greece. Specifically, 100,000 eggs were placed in each of the 2 tanks ($40m^3$), the first of which was supplied with natural seawater and the second with borehole water. Eggs were incubated under natural photoperiod, at 19.5^{o}C and 36 and 38 ppt salinity for borehole and natural sea water, respectively. The trial lasted 56 days after hatching (dph) with the same rearing protocols applied in both tanks. The feeding protocol included the addition of the microalgae *Chlorella sp* in the rearing water from 4 to 15 dph, feeding with enriched rotifers (*Brachionus sp*) from 4 to 18 dph, enriched *Artemia* spp. nauplii from 12 to 36 dph and artificial food (INVE SA, Belgium) from 19 dph. Measurements of pH, O_2 (HQ40D Portable Multi Meter, Hach), CO_2 (CO_2 Portable Carbon Dioxide Analyzer, OxyGuard) and water temperature were performed daily in the two water sources. Random samples of larvae and juvenile fish from both tanks were euthanized with an overdose of tricaine (MS222) and sampled for histology**,** scanning electron microscopy (SEM), micro-CT analysis, Quantitative Real-Time PCR (qPCR) and SDS-PAGE and immunoblot analysis.

2.3 Histology

Three fish from each tank were sampled daily from day 1 to 7, every two days from day 9 to 21 and every five days until day 56 post hatching. The samples were preserved in buffered 4F:1G, containing 4% formaldehyde: 1% gluteraldehyde for at least 24 h (McDowell and Trump, 1976). Subsequently they were dehydrated in gradually increased ethanol solutions (70-96%) and then embedded in glycol methacrylate resin (Technovit 7100, Heraeus Kulzer). Sections of 4 μm were obtained with a microtome (RM 2035, Leica, Germany). After drying, slides were stained with methylene blue/azure II/basic fuchsin according to Bennett et al. (1976) and examined under a light microscope.

2.4 Scanning electron microscopy (SEM)

Three fish from each tank were sampled at 1, 2, 3, 4, 5, 6, 7, 9, 11, 13, 15, 17, 19, 21, 26, 31, 36, 41, 46 and 56 dph fixed in 2.5% glutaraldehyde in 0.1M sodium cacodylate buffer (pH 7.4) for 1 or 2 days (depending on the size of the fish) and then stored in sodium cacodylate buffer at 4°C. The samples were then dehydrated through a graded acetone series, critical point dried and sputter-coated with gold. Samples were viewed using a JEOL JSM-6390LV scanning electronic microscope at 15 kV at the Electron Microscopy Laboratory of the University of Crete.

2.5 Micro-CT

One fish from each tank was sampled at 56 dph, fixed in 10% phosphate-buffered formalin and dehydrated to 70% ethanol for 3 days before scanning. Subsequently, the samples were stained with 0.3% phosphotungstic acid (PTA) in 70% ethanol in order to enhance the contrast between the soft tissues. The micro-CT scans of the samples were performed at the Hellenic Centre for Marine Research (HCMR) using the SkyScan 1172 micro-CT scanner (SkyScan, Bruker, Belgium). This scanner uses a tungsten X-ray source with an anode voltage ranging from 20 to 100 kV, 11 MP CCD camera (4000 × 2672 pixel) and a maximal resolution of < 0.8 μm/pixel. Samples were scanned at a voltage of 80 kV and a current of 124 μA with an aluminum filter of 0.5 mm while the images were acquired at a pixel size of 13.78 μm and exposure time 1435 ms. To minimize the scanning duration, scans were performed for a half rotation of 180^{o}. The projection images acquired during the scanning procedure were reconstructed into cross-section images using the SkyScan's NRecon software (NRecon, Skyscan, Bruker, Belgium) which implements a modified Feldkamp's back-projection algorithm.

2.6 Gene expression of Cathk, TRAP and vATPase

Ten fish of similar weight (1.62±0.33g and 1.69±0.40g from borehole water and natural seawater respectively) from each tank was sampled at 56 dph, frozen in liquid nitrogen and stored at 80°C until analyzed. All fish reared in borehole water had visible signs of the disease as opposed to the fish reared in

157 natural seawater which appeared normal. Head samples were homogenized in 600 µl RLT plus buffer
158 (RNeasy Plus Mini Kit Qiagen, Valencia, USA) using the TissueRuptor (Qiagen, Hilden, Germany).
159 Total RNA was extracted using RNA isolation nucleospin RNA plus (Macherey-Nagel) according to the
160 instructions of the manufacturer. In order to determine RNA yield and purity, measurement of the
161 absorbance at 260 and 280 nm was conducted using the Nanodrop® ND-1000 UV–Vis spectrophotometer
162 (Peqlab, Erlangen, Germany) while the integrity of RNA was tested by electrophoresis in 1% agarose
163 gels. The cDNA was synthesized by reverse transcription of 1µg RNA using the QuantiTect Reverse
164 Transcription kit (Qiagen Inc., CA, USA) according to the manufacturer's instructions. The mRNA
165 expression of genes encoding for tartrate-resistant acid phosphatase (TRAP), Cathepsin K (CathK) and
166 vATPase (primers in **Table 1**) was determined in healthy and CUD-affected head samples with
167 quantitative polymerase chain reaction (qPCR) which was performed on the CFX ConnectTM Real-Time
168 PCR Detection System (Bio-Rad) using the KAPA SYBRR FAST qPCR Kits (KAPA Biosystems, USA).
169 Cycling parameters were as follows: 95°C for 3 min (HotStarTaq DNA Polymerase activation step)
170 followed by 36 cycles at 95°C for 15 s (denaturation step) and 60°C for 30 s (annealing step).
171 Dissociation curve analysis was performed at the end of the cycles to ensure that single amplifications
172 were obtained. A standard curve was constructed for each gene, using four serial dilutions (1:5) of a pool
173 of all cDNA samples by plotting the negative log of the dilution factor against the relative cycle threshold
174 value. Each primer pair was required to have a linear standard curve with an R^2 value above 0.98 and
175 primer amplification efficiency between 95 and 105% in order to be considered suitable for analysis,.
176 Results were evaluated with the Bio-Rad CFX Manager 2.1 software while the data were calculated by
177 the comparative method using Ct values of β-actin as the reference control.
178
179 *2.7 SDS-PAGE and immunoblot analysis*
180 Six fish of similar weight (1.68±0.31 g and 1.65±0.36 g from borehole water and natural seawater
181 respectively) from each tank were sampled at 56 dph, frozen in liquid nitrogen and stored at − 80°C until
182 analyzed. Hsps (Hsp70, Hsp90) and MAPK (p38 MAPK, ERK1/2) members were determined in

183 homogenized head samples according to well established protocols, as described in Antonopoulou et al.,
184 2020, 2014. Briefly, healthy and CUD-affected heads (45-50mg) were homogenized in 3 mlg^{-1} of cold
185 lysis buffer (20 mM Hepes pH 7.5, 20 mM β-glycerophosphate, 50 mM NaF, 2 mM EDTA, 10 mM
186 benzamidine, 0.2 mM Na3VO4, in pH 7, containing 200 μM leupeptin, 300 μM phenyl methyl sulfonyl
187 fluoride (PMSF), 10 μM trans-epoxy succinyl-L-leucylamido-(4- guanidino) butane, 5 mM DTT
188 (dithiothreitol) and 1% v/v Triton X-100). Protein concentration was determined using the BioRad protein
189 assay, a dye-binding assay based on the differential color change of a dye (Coomansie Brilliant Blue G-
190 250) in response to various protein concentrations. Equivalent amounts of protein (50 μg) were separated
191 on 10% (w/v) acrylamide, 0.275% (w/v) bisacrylamide slab gels, and transferred electrophoretically onto
192 nitrocellulose membranes (0.45 μm, Schleicher and Schuell, Keene N.H. 03431, USA). All nitrocellulose
193 membranes were dyed with Ponceau stain to assure a good transfer quality and equal protein loading. The
194 antibodies used were as follows: monoclonal mouse anti-heat shock protein, 70 kDa (Cat. No. H5147,
195 Sigma, Darmstadt, Germany); monoclonal mouse anti-heat shock protein, 90 kDa (Cat. No. H1775,
196 Sigma, Darmstadt, Germany); monoclonal rabbit anti-phospho p44/42 MAPK (Thr202/Tyr204) (Cat. No.
197 4376, Cell Signaling, Beverly, MA, USA); polyclonal rabbit anti-phospho-p38 MAP kinase (Thr180-
198 Tyr182) (Cat. No. 9211, Cell Signaling, Beverly, MA, USA). Finally, bands were detected by enhanced
199 chemiluminescence (Cell Signaling, Beverly, MA, USA) with exposure to Fuji Medical X-ray films.
200 Films were quantified by laser- scanning densitometry (GelPro Analyzer Software, Media Cybernetics).
201
202 *2.8 Metal and element analysis*
203 Nine fish from each tank were sampled at 56 dph, the whole head was dissected from each sample, snap
204 frozen on liquid nitrogen and stored at -80 °C until analysis. The concentrations of 22 metals and
205 elements were determined in the whole head by Inductively Coupled Plasma – Mass Spectrometer (ICP–
206 MS NexION300, PerkinElmer, Shelton, CT, U.S.) following the protocols described in detail by Kalantzi
207 et al. (2013).
208

2.9 Recovery trial

For the recovery trial, a group of 4-month-old meagre (n=500) with visible lesions associated with CUD were transferred from the inland facilities of HCMR in Heraklion to sea cages in the Bay of Souda, Chania. For the next 5 months (once per month), 10 fish were randomly sampled, anesthetized with MS222 and visually examined for external lesions. The farm is certified as an aquaculture facility from the national veterinary authority (code GR94FISH0001). A group of the same population (n=500) was kept in the inland facilities of HCMR in Heraklion and was reared in borehole water for the same period and fish were monitored with the same procedure as with the fish transferred to sea cages.

2.10 Investigation of the effect of CO2 and pH in the development of CUD

A second rearing trial was performed, in order to investigate whether increased CO_2 in borehole water is the aetiological agent responsible for the development of CUD lesions. The eggs used in this trial were obtained by a broodstock maintained at the facilities of the Institute of Marine Biology, Biotechnology and Aquaculture, HCMR, Crete, Greece. In total, 125.000 eggs were placed in each of the 2 tanks ($40m^3$) supplied with natural seawater. In one of the tanks, CO_2 was injected into the seawater before entering the larvae tank, maintaining the pH value at a mean of 7.4, lower to the natural value of pH that had a mean of 8.0, in order to simulate the pH/CO_2 conditions of the borehole water. The trial lasted 60 days dph with the same rearing protocols applied in both tanks. The feeding protocol included the addition of the microalgae *Chlorella sp* in the rearing water from 3 to 15 dph, feeding with enriched rotifers *Brachionus sp* from 3 to 16 dph, enriched *Artemia* spp. nauplii from 11 to 26 dph and artificial food (INVE SA, Belgium) from 18 dph. Measurements of pH, O_2 (HQ40D Portable Multi Meter, Hach), CO_2 (CO_2 Portable Carbon Dioxide Analyzer, OxyGuard) and water temperature were performed daily in the two water sources. Random samples of larvae (n=10) from both tanks were sampled every 7 days and preserved in buffered 4F:1G for histology as described above**.**

3. Results

3.1 Development of the lateral line canals

The first superficial neuromasts appear from the 1 dph both on the head and the trunk of meagre, consisting of the sensory hair cells, the mantle cells and the supporting cells (**Figure 1**). Scanning electron microscopy revealed the presence of two morphological types of superficial neuromasts, round or diamond-shaped, with the latter being larger in size (**Figure 2**).

The morphogenesis of the lateral line canals in the head of meagre is not a synchronized process, however all the canals are completely formed by the 31st dph. The supraorbital is the first canal that begins to form as the first grooves with the submerged neuromasts appear at 9 dph (TL: 5.40 ± 0.27 mm). The ossified canal walls on either side of the neuromast are formed from the 17 dph (TL: 9.48 ± 0.7 mm) while the first neuromasts, enclosed by soft tissue canal roof are observed from the 21 dph (TL: 11.75 ± 0.83 mm) (**Figure 3 & 4)**.

The first grooves of the mandibular canal appear at 11 dph (TL: 6.03 ± 0.39 mm) while the walls of the canal begin to rise on each side of the neuromast at 19 dph (TL: 9.75 ± 1.21 mm) and the first epithelial canal roofs have formed at 21 dph (**Figure 5**). The formation of infraorbital canal starts with the appearance of the first grooves at the 19 dph, the walls of which begin to rise at 21 dph while the first enclosed neuromasts are observed at 26 dph (TL: 18.04 ± 0.69 mm) (**Figure 6**).

3.2 The effect of the borehole water in the development of CUD

The growth of fish in terms of total length and wet weight, reared with different water sources is presented in **Figure 7**. The growth performance of the fish was not affected by the different source of water until 41 dph. On the 44th and 56th dph the weight and the length of the fish reared in the natural seawater was significantly higher than the fish reared in the borehole water.

The temperature of the borehole water remained relatively constant during the rearing trial with a mean value of 20.4±0.5 °C (range 19-21 °C) while in natural seawater the temperature increased from the 35th dph onwards with a mean value of 21.6±1.0 °C (range 20-23 °C).

The dissolved O_2 in natural seawater was 7.27 ± 0.98 mgL^{-1} (range 4.60 - 9.0 mgL^{-1}) and the corresponding value in borehole water was 7.16 ± 1.04 mgL^{-1} (range 5.70 - 9.13 mgL^{-1}). The average pH value in natural seawater was 7.82 ± 0.14 (range 7.54 - 8.01) and in borehole water 7.62 ± 0.15 (range 7.40 - 7.92) while CO_2 was consistently lower in natural seawater with a mean value of 1.56 ± 0.66 mgL^{-1} (range 1.00 - 4.00 mgL^{-1}) compared to borehole water where the mean value was 3.88 ± 0.63 mgL^{-1} (range 3.00 - 5.00 mgL^{-1}) (**Figure 8**).

At the end of the rearing trial (56dph) all fish reared in the tanks supplied with borehole water had visible lesions associated with CUD in comparison with the fish reared in natural sea water (**Figure 9**).

From the comparative histological analysis of meagre reared in borehole and natural seawater no differences were observed until 31 dph. **Figure 10** shows a supraorbital, an infraorbital and a mandibular canal of meagre reared in natural seawater (**Figure 10 A, C, E**) and in borehole water (**Figure 10 B, D, F**) on 56 dph. In meagre reared in natural seawater, the canals were completely developed. Instead, in meagre from borehole water erosion, ulceration and loss of the basal membrane was observed while the neuromasts were exposed to the external environment. The lesions were initially manifested as hydropic swelling and hyperplasia of the epidermis before becoming ulcerative.

The micro-CT scans from the CUD-affected head samples of meagre that was reared in borehole water, revealed that the supraorbital and the infraorbital were the main affected canals while the mandibular had lesions in a smaller extent at least until the 56 dph (Figure 12), whereas, in the samples from the healthy fish that was reared in natural seawater fully formed canals were observed (**Figure 11**).

Scanning electron microscopy of CUD-affected fish revealed the presence of lesions mainly in the nasal cavity and around it where they are normally located the pores of the supraorbital and infraorbital canals while in affected individuals the pore openings have been widened, leaving the canal neuromasts exposed. Moreover, the opening of the nasal cavity in CUD-affected meagre was larger than in healthy individuals however, the olfactory rosette appeared normal. In both healthy and affected individuals, superficial neuromasts located around the opening of the nasal cavity were normal. In addition, the roof of the canal at the area of the supraorbital commissure (SOCom) where the left and

right supraorbital canals join and the roof of the supraorbital canal posterior to SOCom, were absent in the CUD-affected individual, while the exposed canal neuromasts did not appear to be affected at least until 56 dph (**Figure 13, 14**)

3.3 Recovery trial

The transfer of 4-month meagre with lesions associated with CUD from borehole water to natural seawater showed that CUD is a reversible condition as after 5 months in natural sea water the meagre showed almost 100% healing of the lesions as assessed by macroscopic observations. On the other hand, the group of fish that was kept in the inland facilities of HCMR and was reared in borehole water for the same period showed deterioration of the condition with severe ulceration in the head area. (**Figure 15**)

3.4 Expression of genes and proteins in healthy and CUD-affected meagre

The expression profile of CathK, TRAP and vATPase in the head tissues of the fish reared in different water sources was significantly different at the end of the rearing trial (56 dph) (**Figure 16**). In particular, cathepsin K and TRAP expression was 2.7 and 2.1 times higher, respectively, in the CUD-affected fish of the borehole water group compared to the healthy fish of the natural seawater group ($t(17)=2.26$, $p=0.037$ for cathepsin K and $t(17)=2.41$, $p=0.028$ for TRAP). The expression of vATPase did not exhibit significant differences between the fish from the two water sources ($t(17)= -.219$, $p=0.830$)

The relative protein expression of Hsp90, Hsp70, phospho p38 MAPK and phospho p44/42 MAPK in the head tissues of healthy and CUD-affected fish which were reared in natural seawater and borehole water respectively, was significantly different at the end of the rearing trial (56 dph) (**Figure 17**). In particular, the Hsp70 and Hsp90 was 4 and 4.9 times higher, respectively, in the CUD-affected fish of the borehole water compared to the healthy fish of the seawater ($t(10) = 51.14$, $p = 0,000$ for Hsp70 and $t(10) = 21.01$, $p = 0,000$ for Hsp90). Moreover, CUD-affected fish exhibited increased phosphorylation of p38 MAPK (3.2 times higher, $t(10) = 30.03$, $p = 0.000$) and p44/42 MAPK (2.5 times higher, $t(10) = 26.36$, $p = 0.000$) compared to the healthy meagre.

3.5 Metal and element concentrations in healthy and CUD-affected meagre

Mean elemental concentrations in the heads of healthy and CUD-affected meagre reared in natural seawater and borehole water respectively are summarized in **Table 2** The CUD-affected meagre were found to have significantly higher concentrations of Lithium (Li), Chromium (Cr), Cobalt (Co), Copper (Cu) and Barium (Ba) compared to healthy fish ($p<0.05$). Moreover, Aluminum (Al), Vanadium (V), Cadmium (Cd), Caesium (Cs) and Lead (Pb) were detected only in fish reared in borehole water.

3.6 The effect of the CO_2 and pH in the development of CUD

At the end of the second rearing trial (60 dph) no statistically significant differences were observed on the average weight and length of the fish that were reared in natural seawater and natural seawater + CO_2 ($t(118)=1.02$, $p=0.309$ for the weight and $t(118)=1.89$, $p=0.062$ for the length). Specifically, the fish reared in natural seawater had an average weight of 2.00 ± 0.65 g and an average length of 5.37 ± 0.61 cm, while those reared in natural seawater+CO_2 had a mean final weight 2.10 ± 0.50 g and mean final length 5.55 ± 0.39 cm.

The temperature in both tanks showed a similar upward trend during the experiment with the mean value of 24.1 ± 1.32 °C (range 20.4-26.9 °C) in the tank that was supplied with natural seawater and 23.95 ± 1.39 °C (range 20.3-26.7 °C) in the tank that was supplied with natural seawater+CO_2.

The dissolved O_2 in the tank with the natural seawater was 7.79 ± 1.34 mgL^{-1} (range 5.03 - 9.94 mgL^{-1}) and the corresponding value in the natural seawater+CO_2 water was 7.85 ± 1.49 mgL^{-1} (range 4.90 – 11.00 mgL^{-1}).

The mean pH value in natural seawater was 7.98 ± 0.13 (range 7.75 - 8.66) and in natural seawater+CO_2 7.36 ± 0.19 (range 6.72 - 7.83) while CO_2 was consistently lower in natural seawater tank with a mean value of 1.32 ± 0.74 mgL^{-1} (range 0.00 - 3.00 mgL^{-1}) compared to natural seawater+CO_2 tank where the mean value was 4.43 ± 0.65 mgL^{-1} (range 3.00 - 6.00 mgL^{-1}) (**Figure 18**).

Although the CO_2 and pH in the tank with the natural seawater + CO_2 were adjusted to replicate the conditions of the borehole water, at the end of the rearing trial (60 dph) none of the fish that reared in this water had visible lesions associated with CUD as shown in **Figure 19**. Histological analysis of head samples from meagre reared in natural seawater+CO_2 confirmed the non-development of CUD-related lesions, as the lateral canal were found to be fully formed and normal (**Figure 20**).

4. Discussion

The aim of this study was to investigate the development of CUD in meagre by a comparative study of two populations reared parallelly in tanks supplied with natural seawater or borehole seawater. From the specific comparative rearing trial, it was confirmed that the use of borehole water leads to the development of lesions related to CUD in the entire farmed meagre population. The ulcerative lesions in the head became visible macroscopically in fish at 56 dph (TL: 4.37 ± 0.11 cm), while CUD was found to be a reversible pathological condition as the transport of affected individuals in natural sea water led to complete healing of the lesions within a period of 5 months. These results are in accordance with other reported cases of CUD, both in freshwater and marine fish species. In the Australian freshwater fish Murray cod, *Maccullochella peelii peelii* the first gross signs appeared approximately three weeks after exposure to groundwater as enlargement of the pores of the head and trunk canals. Progressively, the elongated pores began to coalesce, resulting in exposure of the bed of the canal and finally all the canal beds were exposed while ulceration on the head started to extend into surrounding areas. Similar to meagre, it was shown that when CUD-affected Murray cod were transferred to river water, the majority of the fish were structurally recovered after a period of 8-10 weeks (Baily et al., 2005). Concerning marine fish species, the first lesions of CUD in sharpsnout seabream were observed at 70 dph while at 130 dph all fish that were reared in borehole water had bilateral grooves at the area of the lateral line canals. The transportation of the affected fish in natural sea water led to the recovery of the lesions over a period of about 4 months (Katharios et al., 2011).

In contrast to Murray cod, in which CUD led to reduced growth rate and increased mortality, no mortality was observed in CUD-affected meagre. The relatively reduced growth that was observed in CUD-affected meagre is probably related to the lower temperature of the borehole water in comparison to the natural sea water (20.4 ± 0.5 °C and 21.6 ± 1.0 °C, respectively) as it is known that increasing the temperature up to 26 °C has a beneficial effect on the growth of the meagre (Antonopoulou et al., 2020; Chatzifotis et al., 2018).

The results from histology, SEM and μ-CT confirmed that the lesions in meagre were limited to the lateral line organ in the head and in the nasal cavity which is in agreement with the conclusions of Baily et al. (2005) for Murray cod and of Katharios et al. (2011) for sharpsnout seabream.

From the histological comparative analysis, no differences were observed up to 36 dph between the groups reared in natural seawater and in borehole water respectively, with the development of the lateral line canals in the head occurring normally in both groups. The cranial lateral line canals of meagre like most teleost bony fish (Webb, 2014, 2013) are narrow and well-ossified. The development of the lateral line canals is an asynchronous process both within the same canal and between the different canals, with the supraorbital and the mandibular canals being the first to begin forming, followed by the infraorbital (Webb, 2014). This was also confirmed in the case of meagre, as the supraorbital and the mandibular canals starts to form when the fish are 5.40 ± 0.27 mm and 6.03 ± 0.39 mm, respectively while the infraorbital canal starts to develop when the fish are 9.75 ± 1.21 mm and all canals are fully formed when the fish are 19.3 ± 1.27 mm. The development of the lateral cranial canals has been studied mainly in various species of cichlids (*Amatitlania nigrofasciata*, *Labeotropheus fuelleborni*, *Maylandia zebra*, *Aulonocara baenschi*, *Aulonocara stuartgranti* and *Tramitichromis* sp) and does not differ significantly compared to meagre. In all cases the onset of canal formation is observed when the fish are 5 - 8 mm in length while the completion of the formation is observed when the fish are 16 - 22 mm (Becker et al., 2016; Tarby and Webb, 2003; Webb, 2014). In contrast to both meagre and the various species of cichlids, the development of lateral canal canals in zebrafish (*Danio rerio*) appears to be delayed as the first submerged neuromasts of the supraorbital and the mandibular canals appear when the fish are 10 mm

388 and 11.5 mm respectively, however, their closure is observed when the fish is 22 mm in length (Webb
389 and Shirey, 2003).
390 Histologically, the first lesions related to CUD in meagre were observed from 36 dph onwards.
391 The lesions were initially manifested as hydropic swelling and hyperplasia of the epidermis before
392 becoming ulcerative leaving the canal neuromasts exposed. The neuromasts did not appear to be affected
393 by CUD at least until the age of 56 dph. In murray cod, the first lesions of CUD were observed
394 histologically 3 weeks after exposure of the fish to borehole water, as marked hyperplasia and necrosis.
395 Two weeks later, the tissue above the canals was completely necrotic, however as in the case of meagre,
396 no degeneration of the exposed neuromasts was observed (Baily et al., 2005). In CUD-affected
397 sharpsnout seabream, the histological examination revealed the presence of ulcers in the cranial lateral
398 line canals while the roof of the canals was always absent leaving the canal neuromasts exposed. In
399 contrast to meagre and to murray cod the exposed neuromasts of sharpsnout seabream appeared either
400 normal or degenerated and necrotic (Katharios et al., 2011). In the case of sharpsnout seabream the nasal
401 cavity was affected from CUD which was also observed and in meagre. However, in the sharpsnout
402 seabream the olfactory rosette was also damaged (Katharios et al., 2011) which was not observed in
403 meagre.
404 In either cases of meagre, murray cod and sharpsnout seabream there is evidence that the
405 development of CUD is directly linked with the use of groundwater, which is reinforced by the fact that
406 the condition is reversed by transporting the fish in natural sea or fresh water. However, the actual
407 causative agent of CUD is unknown in all cases. It is noteworthy that the pH was lower and CO_2 higher in
408 borehole water in comparison with natural seawater. High levels of CO_2 in rearing water of fish leads to a
409 decrease in pH of their extracellular environment. The decrease of pH in the extracellular environment is
410 one of the factors that can lead to the activation of osteoclasts (Arnett, 2008; Yuan et al., 2016), which in
411 collaboration with osteoblasts, participate in the remodeling of the bones that contain the lateral line
412 canals as the fish grows in size (Wada et al., 2014; Webb, 2013). An imbalance between osteoclasts and
413 osteoblasts could lead to the lesions seen in the fish, located exclusively in the lateral line canals. The

tartate-resistant acid phosphatase (TRAP) is the most widely used marker enzyme for the identification of osteoclasts and with the cysteine proteinase cathepsin K (CathK) are being used as molecular markers of bone resorption (Azuma et al., 2007; Costa et al., 2011; Minkin, 1982). Moreover, the vacuolar-type proton pumping ATPases (V-ATPase) are important for the normal function of these enzymes as they are responsible for the acidic pH of the bone resorption lacunae which is formed between the osteoclast plasma membrane and the bone surface through secretion of protons (Futai et al., 2019). Gene expression of TRAP, cathK, and v-ATPase showed that the CUD-affected meagre had significantly higher levels of TRAP and cathK compared to healthy meagre while v-ATPase levels were higher but not statistically significant compared to healthy individuals. These results indicate that there is an increased osteoclastic activity in the head of the CUD-affected meagre. In mammals it has been shown that increased osteoclastic activity could lead to an imbalance in bone remodeling which promotes resorption resulting to skeletal diseases such as osteoporosis, rheumatoid arthritis, periodontal disease, multiple myeloma and metastatic cancers (Boyle et al., 2003; Rodan and Martin, 2000). Moreover, in accordance with the results from meagre, preliminary results from CUD-affected sharpsnout seabream using enzyme histochemistry has shown increased TRAP activity at the area of the lesions compared to normal samples (Katharios et al., 2011). The increased osteoclastic activity in the head area of CUD-affected meagre reared in borehole water compared to those reared in natural seawater was also confirmed by the comparative expression of phospho p38 MAPKs and phospho p44/42, since in healthy fish reared in natural seawater their levels were significantly lower. The higher expression of MAPKs in CUD-affected fish can be explained by the fact that both p38 MAPKs and p44/42 are activated by the binding of RANKL to the RANK receptor of osteoclasts, which in turn leads to the downstream activation of transcription factors controlling the expression of the genes encoding for TRAP and CathK, in areas where bone resorption occurs (Boyle et al., 2003; Lee et al., 2018). Hsp70 and Hsp90 were also overexpressed in the CUD-affected individuals compared to the healthy fish, which enhances the increased osteoclastic activity as Hsp70 induces osteoclastic bone resorption via the RANKL / RANK pathway, while even though the role of Hsp90 in

osteoclastogenesis is controversial it has been shown that it can induce the expression of osteoclast-associated genes (Hang et al., 2018).

Based on the results from the comparative rearing of meagre in natural seawater and borehole water, the second larval rearing trial was performed in order aiming to test whether increased CO_2 concentration is the aetiological agent for the development of CUD lesions. This trial was designed in order to replicate the pH and CO_2 conditions of the borehole water without including any other chemical or environmental factor. After macroscopic examination and histological analysis, it was revealed that none of the fish reared in the natural seawater where CO_2 was added showed any lesions related to CUD. The lack of the lesions in the head of the fish suggests that neither the increased CO_2 nor the consequently reduced pH are the factors affecting the development of CUD.

The results from the metal analysis of healthy meagre reared in natural seawater and CUD-affected meagre reared in borehole water showed that fish with lesions had significantly higher levels of Li, Cr, Co, Cu and Ba in relation to healthy individuals. In addition, Al, V, Cd, Cs and Pb were detected only in CUD-affected fish while in healthy individuals they were below detectable limits. Metals can be categorized as biologically essential and nonessential. The nonessential metals (e.g., Al, V, Cd, Pb, Ba) which have no proven biological function can become extremely toxic for organisms due to their persistence and their tendency to bioaccumulate (Amoussou et al., 2019; Carvalho et al., 2005; Tarley et al., 2001). On the other hand, essential metals (e.g., Cu, Zn, Cr, Co), have a known biological role, and they can become toxic either at deficiencies or at high concentrations (Kennedy, 2011). In general, metals can affect multiple physiological systems of fish while toxicity depends on metal form, bioavailability, toxicokinetics and toxicodynamics (Kennedy, 2011; Sfakianakis et al., 2015). Heavy metals in the water can cause reduction of the survival and the growth of fish larvae, behavioral anomalies or structural damages (Stominska and Jezierska, 2000). More specifically, metals can reduce calcium uptake and bone calcium accumulation leading to changes in bone properties and can induce disturbances of neuro-muscular transmission leading to skeletal deformities (Hassanain et al., 2012). It was reported that exposure of freshwater fish to Hg and Cd leads to a disturbed calcium metabolism, resulting in

hypocalcemia and anomaly of the bone. Both metals, first influence osteoclastic activities under acute exposure and then inhibit osteoblastic activities under long-time exposure (Suzuki et al., 2004). Moreover, carp larvae exposed to Pb, developed scoliosis, while Cu caused inhibition of skeletal ossification which might have resulted from impaired ionic regulation. In addition, both metals caused reduction of the fish survival and the growth rates (Stominska and Jezierska, 2000). Disturbance of bone ossification was also reported in Nile tilapia after exposure to Pb (Hassanain et al., 2012). In addition to fish, it was reported that exposure of chick femur culture to Zn and Cd led to decreased mineralization of bone, with or without suppression of matrix formation while exposure to Zn and Cu caused decreased mineralization and matrix formation (Toshiyuki et al., 1991). Moreover, it was found that Zn is an extremely potent inhibitor of rat osteoclasts in vitro, since significant inhibition of resorption was reported at concentrations as low as 10^{-14} M (Moonga and Dempster, 1995). In the case of meagre, despite the differences between healthy and CUD affected fish, the values observed are within the range of values reported for other fish species, including gilthead seabream and European seabass when lesions are absent (El-Moselhy et al., 2014; Kalantzi et al., 2016, 2013). On the other hand, it has been reported that Cu concentrations above 1mg L^{-1} can cause damage to the epithelium of the lateral canal of *Fundulus hereroclitus* while in some cases canal neuromasts were also affected (Eisler and Gardner, 1973). It has been shown that metals such as Cu are toxic to the peripheral sensory systems of fish and other aquatic organisms by reducing the physiological response or at higher concentrations by cell death of the olfactory and mechanosensory neurons (Linbo et al., 2009). Moreover, lateral line dysfunction was reported after exposure of zebrafish embryos to Cu (68 and 244 μg Cu L^{-1}). The copper-exposed larvae showed fewer functional neuromasts which was associated with a reduced ability of orientation in a current (Johnson et al., 2007). Neuromasts cellular damage, apoptosis, and loss of hair cell markers were also reported in zebrafish after exposure to sub-lethal concentrations of waterborne copper while other metals such as Zn, Fe, Ag, Mn, Co, Cd and Sn, did not show the same effects (Hernández et al., 2006).The concentration of Cu in the head of CUD-affected meagre was 1.70 ± 0.51 mg kg^{-1}, while in healthy fish it was significantly lower (0.85 ± 0.25 mg kg^{-1}) suggesting that Cu could be one of the factors

leading to the development of CUD. Moreover, in the study of CUD in the sharpsnout seabream the concentrations of Ni, Pb, Zn and Cu were higher in the borehole water than in the natural seawater, however these levels were within the acceptable limits for marine aquaculture and much lower than the toxic limits (Katharios et al., 2011). Nevertheless, metal toxicity as a causative factor for the development of CUD cannot be ruled out because of the lower pH of the borehole water and the longer exposure times of the fish and therefore it should be further studied in the future as environmental parameters and interactions among various metals may affect their toxicity to fish (Sfakianakis et al., 2015).

Although the disease is directly associated with the use of borehole water, the causative agent is still unknown for meagre, as well as for Murray cod and sharpsnout seabream. For all species the lesions resolve when the fish are transferred to natural freshwater or seawater (Baily et al., 2005; Katharios et al., 2011). Furthermore, for Murray cod, Schultz et al. (2011) found that the retention of groundwater into a vegetated earthen pond or in a tank containing biofilms growing on an artificial macrophyte for 72 h prevents the development of CUD. Thus, it is recommended to avoid borehole seawater for the rearing of meagre if natural sea water sources are available and to pay careful attention to the water quality of the source of the water used. Alternatively, the residence time of meagre in borehole water should be reduced to the minimum necessary, and fish should be moved to natural seawater (e.g. in sea cages) as soon as possible once the nursery phase is completed, in order to allow the tissue regeneration process to complete before marketing the fish.

5. Acknowledgments

Funding was provided for this project from The European Union's Seventh Framework Programme for research, technological development and demonstration (KBBE-2013-07 single stage, GA 603121, DIVERSIFY).

6. References

Amoussou, N., Marengo, M., Durieux, E.D.H., Douny, C., Scippo, M.L., Gobert, S., 2019. Trace

Elements and Fatty Acid Profile of *Argyrosomus regius* (Asso, 1801) from Mediterranean Aquaculture. Biol. Trace Elem. Res. https://doi.org/10.1007/s12011-019-01925-x

Antonopoulou, E., Chatzigiannidou, I., Feidantsis, K., Kounna, C., Chatzifotis, S., 2020. Effect of water temperature on cellular stress responses in meagre (*Argyrosomus regius*). Fish Physiol. Biochem. 46, 1075–1091. https://doi.org/10.1007/s10695-020-00773-0

Antonopoulou, E., Kousidou, E., Tserga, E., Feidantsis, K., Chatzifotis, S., 2014. Dietary lipid levels in meagre (*Argyrosomus regius*): Effects on biochemical and molecular indicators of liver. Aquaculture 428–429, 265–271. https://doi.org/10.1016/j.aquaculture.2014.03.024

Arnett, T.R., 2008. Extracellular pH Regulates Bone Cell Function. J. Nutr. 138, 415S-418S. https://doi.org/10.1093/jn/138.2.415s

Azuma, K., Kobayashi, M., Nakamura, M., Suzuki, N., Yashima, S., Iwamuro, S., Ikegame, M., Yamamoto, T., Hattori, A., 2007. Two osteoclastic markers expressed in multinucleate osteoclasts of goldfish scales. Biochem. Biophys. Res. Commun. 362, 594–600. https://doi.org/10.1016/j.bbrc.2007.08.010

Baily, J.E., Bretherton, M.J., Gavine, F.M., Ferguson, H.W., Turnbull, J.F., 2005. The pathology of chronic erosive dermatopathy in Murray cod, *Maccullochella peelii peelii* (Mitchell). J. Fish Dis. 28, 3–12. https://doi.org/10.1111/j.1365-2761.2004.00586.x

Becker, E.A., Bird, N.C., Webb, J.F., 2016. Post-embryonic development of canal and superficial neuromasts and the generation of two cranial lateral line phenotypes. J. Morphol. 277, 1273–1291. https://doi.org/10.1002/jmor.20574

Bennett, H.S., Wyrick, A.D., Lee, S.W., McNeil, J.H., 1976. Science and Art in Preparing Tissues Embedded in Plastic for Light Microscopy, with Special Reference to Glycol Methacrylate, Glass Knives and Simple Stains. Stain Technol. 51, 71–97. https://doi.org/10.3109/10520297609116677

Bleckmann, H., Zelick, R., 2009. Lateral line system of fish. Integr. Zool. 4, 13–25.

Boyle, W.J., Simonet, W.S., Lacey, D.L., 2003. Osteoclast differentiation and activation. Nature 423, 337–342. https://doi.org/10.1038/nature01658

543 Carvalho, M.L., Santiago, S., Nunes, M.L., 2005. Assessment of the essential element and heavy metal
544 content of edible fish muscle. Anal. Bioanal. Chem. 382, 426–432. https://doi.org/10.1007/s00216-
545 004-3005-3
546 Chatzifotis, S., Clavero, S., Kounna, C., Soumalevris, A., Feidantsis, K., Antonopoulou, E., 2018. Effects
547 of long-term feed deprivation on body weight loss, muscle composition, plasma metabolites, and
548 intermediate metabolism of meagre (*Argyrosomus regius*) under different water temperatures. Fish
549 Physiol. Biochem. 44, 527–542. https://doi.org/10.1007/s10695-017-0451-3
550 Corrales, J., Ullal, A., Noga, E.J., 2009. Lateral line depigmentation (LLD) in channel catfish, *Ictalurus*
551 *punctatus* (Rafinesque). J. Fish Dis. 32, 705–712. https://doi.org/10.1111/j.1365-2761.2009.01069.x
552 Costa, A.G., Cusano, N.E., Silva, B.C., Cremers, S., Bilezikian, J.P., 2011. Cathepsin K: Its skeletal
553 actions and role as a therapeutic target in osteoporosis. Nat. Rev. Rheumatol. 7, 447–456.
554 https://doi.org/10.1038/nrrheum.2011.77
555 Eisler, R., Gardner, G.R., 1973. Acute toxicology to an estuarine teleost of mixtures of cadmium, copper
556 and zinc salts. J. Fish Biol. 5, 131–142. https://doi.org/10.1111/j.1095-8649.1973.tb04441.x
557 El-Moselhy, K.M., Othman, A.I., Abd El-Azem, H., El-Metwally, M.E.A., 2014. Bioaccumulation of
558 heavy metals in some tissues of fish in the Red Sea, Egypt. Egypt. J. Basic Appl. Sci. 1, 97–105.
559 https://doi.org/10.1016/j.ejbas.2014.06.001
560 Futai, M., Sun-Wada, G.-H., Wada, Y., Matsumoto, N., Nakanishi-Matsui, M., 2019. Vacuolar-type
561 ATPase: A proton pump to lysosomal trafficking. Proc. Japan Acad. Ser. B 95, 261–277.
562 https://doi.org/10.2183/pjab.95.018
563 Gratzek, J.B., 1988. Parasites Associated with Ornamental Fish. Vet. Clin. North Am. Small Anim. Pract.
564 18, 375–399. https://doi.org/10.1016/S0195-5616(88)50038-4
565 Hang, K., Ye, C., Chen, E., Zhang, W., Xue, D., Pan, Z., 2018. Role of the heat shock protein family in
566 bone metabolism. Cell Stress Chaperones 23, 1153–1164. https://doi.org/10.1007/s12192-018-0932-
567 z
568 Hassanain, M.A., Abbas, W.T., Ibrahim, T.B., 2012. Skeletal Ossification Impairment in Nile Tilapia

(*Oreochromis niloticus*) after Exposure to Lead Acetate. Pakistan J. Biol. Sci. 15, 729–735. https://doi.org/10.3923/pjbs.2012.729.735

Hernández, P.P., Moreno, V., Olivari, F.A., Allende, M.L., 2006. Sub-lethal concentrations of waterborne copper are toxic to lateral line neuromasts in zebrafish (*Danio rerio*). Hear. Res. 213, 1–10. https://doi.org/10.1016/j.heares.2005.10.015

Ingram, B.A., Gavine, F., Lawson, P., 2004. Diseases and health management in intensive Murray cod aquaculture, in: Ingram, B.A., De Silva, S.S. (Eds.), Development of Intensive Commercial Aquaculture Production Technology for Murray Cod. Primary Industries Research Victoria, Marine and Freshwater Systems, Department of Primary Industries, Queenscliff, Victoria, pp. 129–146.

Johnson, A., Carew, E., Sloman, K.A., 2007. The effects of copper on the morphological and functional development of zebrafish embryos. Aquat. Toxicol. 84, 431–438. https://doi.org/10.1016/j.aquatox.2007.07.003

Kalantzi, I., Black, K.D., Pergantis, S.A., Shimmield, T.M., Papageorgiou, N., Sevastou, K., Karakassis, I., 2013. Metals and other elements in tissues of wild fish from fish farms and comparison with farmed species in sites with oxic and anoxic sediments. Food Chem. 141, 680–694. https://doi.org/10.1016/j.foodchem.2013.04.049

Kalantzi, I., Pergantis, S.A., Black, K.D., Shimmield, T.M., Papageorgiou, N., Tsapakis, M., Karakassis, I., 2016. Metals in tissues of seabass and seabream reared in sites with oxic and anoxic substrata and risk assessment for consumers. Food Chem. 194, 659–670. https://doi.org/https://doi.org/10.1016/j.foodchem.2015.08.072

Katharios, P., Papadaki, M., Ternengo, S., Kantham, P.K., Zeri, C., Petraki, P.E., Divanach, P., 2011. Chronic ulcerative dermatopathy in cultured marine fishes. Comparative study in sharpsnout sea bream, *Diplodus puntazzo* (Walbaum). J. Fish Dis. 34, 459–474. https://doi.org/10.1111/j.1365-2761.2011.01257.x

Kennedy, C.J., 2011. TOXICOLOGY | The Toxicology of Metals in Fishes, in: Encyclopedia of Fish Physiology. Elsevier, pp. 2061–2068. https://doi.org/10.1016/B978-0-12-374553-8.00236-7

595 Lee, K., Seo, I., Choi, M.H., Jeong, D., 2018. Roles of mitogen-activated protein kinases in osteoclast
596 biology. Int. J. Mol. Sci. 19. https://doi.org/10.3390/ijms19103004
597 Linbo, T.L., Baldwin, D.H., McIntyre, J.K., Scholz, N.L., 2009. Effects of water hardness, alkalinity, and
598 dissolved organic carbon on the toxicity of copper to the lateral line of developing fish. Environ.
599 Toxicol. Chem. 28, 1455–1461. https://doi.org/10.1897/08-283.1
600 McDowell, E.M., Trump, B.F., 1976. Histologic fixatives suitable for diagnostic light and electron
601 microscopy. Arch. Pathol. Lab. Med. 100, 405–414.
602 Minkin, C., 1982. Bone acid phosphatase: Tartrate-resistant acid phosphatase as a marker of osteoclast
603 function. Calcif. Tissue Int. 34, 285–290. https://doi.org/10.1007/BF02411252
604 Mogdans, J., Kröther, S., Engelmann, J., 2004. Neurobiology of the Fish Lateral Line: Adaptations for the
605 Detection of Hydrodynamic Stimuli in Running Water. Senses Fish 265–287.
606 https://doi.org/10.1007/978-94-007-1060-3_12
607 Moonga, B.S., Dempster, D.W., 1995. Zinc is a potent inhibitor of osteoclastic bone resorption in vitro. J.
608 Bone Miner. Res. 10, 453–457. https://doi.org/10.1002/jbmr.5650100317
609 Morrison, C.M., O'Neil, D., Wright, J.R., 2007. Histopathology of "hole-in-the-head" disease in the Nile
610 Tilapia, *Oreochromis niloticus*. Aquaculture 273, 427–433.
611 Noga, E.J., 2010. Fish Disease: Diagnosis and Treatment, Second Edition, Wiley-Blackwell.
612 https://doi.org/10.1002/9781118786758
613 Rigos, G., Katharios, P., 2010. Pathological obstacles of newly-introduced fish species in Mediterranean
614 mariculture: A review. Rev. Fish Biol. Fish. 20, 47–70.
615 Rodan, G.A., Martin, T.J., 2000. Therapeutic Approaches to Bone Diseases. Science (80-.). 289, 1508–
616 1514. https://doi.org/10.1126/science.289.5484.1508
617 Schultz, A.G., Healy, J.M., Jones, P.L., Toop, T., 2008. Osmoregulatory balance in Murray cod,
618 *Maccullochella peelii peelii* (Mitchell), affected with chronic ulcerative dermatopathy. Aquaculture
619 280, 45–52. https://doi.org/10.1016/j.aquaculture.2008.04.011
620 Schultz, A.G., Shigdar, S.L., Jones, P.L., Ward, A.C., Toop, T., 2011. Groundwater pre-treatment

prevents the onset of chronic ulcerative dermatopathy in juvenile Murray cod, *Maccullochella peelii peelii* (Mitchell). Aquaculture 312, 19–25. https://doi.org/10.1016/j.aquaculture.2010.12.013

Sfakianakis, D.G., Renieri, E., Kentouri, M., Tsatsakis, A.M., 2015. Effect of heavy metals on fish larvae deformities: A review. Environ. Res. 137, 246–255. https://doi.org/10.1016/j.envres.2014.12.014

Soares, F., Roque, A., Gavaia, P.J., 2018. Review of the principal diseases affecting cultured meagre (*Argyrosomus regius*). Aquac. Res. 49, 1373–1382. https://doi.org/10.1111/are.13613

Stominska, I., Jezierska, B., 2000. The effect of heavy metals on postembryonic development of common carp, *Cyprinus carpio* L. Arch. Polish Fish. 8, 119–128.

Suzuki, N., Yamamoto, M., Watanabe, K., Kambegawa, A., Hattori, A., 2004. Both mercury and cadmium directly influence calcium homeostasis resulting from the suppression of scale bone cells: The scale is a good model for the evaluation of heavy metals in bone metabolism. J. Bone Miner. Metab. 22, 439–446. https://doi.org/10.1007/s00774-004-0505-3

Tarby, M.L., Webb, J.F., 2003. Development of the supraorbital and mandibular lateral line canals in the cichlid, *Archocentrus nigrofasciatus*. J. Morphol. 255, 44–57. https://doi.org/10.1002/jmor.10045

Tarley, C.R.T., Coltro, W.K.T., Matsushita, M., De Souza, N.E., 2001. Characteristic levels of some heavy metals from Brazilian canned sardines (*Sardinella brasiliensis*). J. Food Compos. Anal. 14, 611–617. https://doi.org/10.1006/jfca.2001.1028

Toshiyuki, K., Masakazu, T., Tatsuro, M., Hiroshi, K., Fumitomo, K., 1991. Interaction between cadmium and copper on ossification of embryonic chick bone in tissue culture. Toxicol. Lett. 55, 255–262. https://doi.org/10.1016/0378-4274(91)90005-Q

Wada, H., Iwasaki, M., Kawakami, K., 2014. Development of the lateral line canal system through a bone remodeling process in zebrafish. Dev. Biol. 392, 1–14. https://doi.org/10.1016/j.ydbio.2014.05.004

Webb, J.F., 2014. Lateral Line Morphology and Development and Implications for the Ontogeny of Flow Sensing in Fishes, in: Flow Sensing in Air and Water. Springer Berlin Heidelberg, Berlin, Heidelberg, pp. 247–270. https://doi.org/10.1007/978-3-642-41446-6_10

Webb, J.F., 2013. Morphological Diversity, Development, and Evolution of the Mechanosensory Lateral

Line System, in: Coombs, S., Bleckmann, H., Fay, R., Popper, A. (Eds.), The Lateral Line System. pp. 17–72. https://doi.org/10.1007/2506_2013_12

Webb, J.F., 1989. Gross morphology and evolution of the mechanoreceptive lateral-line system in teleost fishes. Brain. Behav. Evol. https://doi.org/10.1159/000115896

Webb, J.F., Shirey, J.E., 2003. Postembryonic development of the cranial lateral line canals and neuromasts in zebrafish. Dev. Dyn. 228, 370–385. https://doi.org/10.1002/dvdy.10385

Yuan, F.L., Xu, M.H., Li, X., Xinlong, H., Fang, W., Dong, J., 2016. The roles of acidosis in osteoclast biology. Front. Physiol. 7, 1–8. https://doi.org/10.3389/fphys.2016.00222

Figure 1. **A:** Superficial neuromast on the head of 1 dph meagre (*Argyrosomus regius*). **B:** Superficial neuromast on the body of 6 dph meagre (TL: 4.05 ± 0.08 mm). **C:** Higher magnification of superficial neuromast on the body of 11 dph meagre (TL: 6.03 ± 0.39 mm) where is visible the sensory cells, the mantle cells and the supporting cells. Stain with methylene blue/azure II/basic fuchsin.

Figure 2. SEM micrographs of meagre's (*Argyrosomus regius*) head. **A:** Diamond shaped superficial neuromast on the head (3 dph – TL:3.54 ± 0.00 mm). **B:** Round shaped superficial neuromast on the head (5 dph – TL: 3.68 ± 0.00 mm). **C:** Diamond shaped superficial neuromast on the head (17 dph – TL: 9.48 ± 0.7 mm). **D:** Higher magnification of picture C with the stereocilium and the kinocilium of the hair cells. Double-headed arrows show hair cell orientation. S: stereocilia, K: kinocilium

Figure 3. Development of the subraobrital canal of meagre (*Argyrosomus regius*). **A:** Longitudinal section of a presumptive canal neuromast sitting on the epithelial surface (5 dph – TL: 3.68 ± 0.00 mm) (red arrow). **B:** Cross section of the neuromast in canal groove (11 dph – TL: 6.03 ± 0.39 mm). **C:** Cross section of the development of the epithelial canal roof with the enclosed neuromast (19 dph – TL: 9.75 ± 1.21 mm). **D-H:** Cross sections of the fully formed supraorbital canal as it is distributed from the anterior to the posterior part of the head (46 dph – TL: 41.78 ± 0.87 mm). b: brain, cr: canal roof, cw: canal walls, e: eye, er: epithelial roof, nm: neuromast. Stain with methylene blue/azure II/basic fuchsin.

Figure 4. SEM micrographs with the development of the supraorbital canal of meagre (*Argyrosomus regius*). **A:** Superficial neuromasts over the eye of meagre (5 dph – TL: 3.68 ± 0.00 mm) (red arrows). **B:** Neuromasts in epithelial depressions (red arrows) over the eye of meagre (17 dph – TL: 9.48±0.7 mm). **C:** Grooves of partially enclosed supraorbital canals with one formed pore (red arrow) (21 dph – TL: 11.75 ± 0.83 mm). **D:** 31dph meagre (TL: 19.30 ± 1.27 mm) with enclosed canals on the head. N: nostril

Figure 5. Development of the mandibular canal of meagre (*Argyrosomus regius*). **A:** Longitudinal section of a presumptive canal neuromast sitting on the epithelial surface (7 dph – TL: 4.08 ± 0.03 mm) (red arrow). **B:** Cross section of the neuromast in canal groove (17 dph – TL: 9.48 ± 0.70 mm). **C:** Cross section of the epithelial canal roof with the enclosed neuromast (21 dph – TL: 11.75 ± 0.83 mm). **D:** Cross sections of the fully formed mandibular canal (56 dph – TL: 46.8 ± 0.18 mm). cr: canal roof, cw: canal walls, e: eye, er: epithelial roof, nm: neuromast. Stain with methylene blue/azure II/basic fuchsin.

Figure 6. Development of the infraorbital canal of meagre (*Argyrosomus regius*). **A:** Horizontal section of a presumptive canal neuromast sitting on the epithelial surface (4 dph – TL: 3.53 ± 0.00 mm) (red arrow). **B:** Cross section of the neuromast in canal groove (21 dph – TL: 11.75 ± 0.83 mm). **C:** Cross section of the epithelial canal roof with the enclosed neuromast (26 dph – TL: 18.04 ± 0.69 mm). **D:** Cross sections of the fully formed infraorbital canal (46 dph – TL: 41.78 ± 0.87 mm). cr: canal roof, cw: canal walls, e: eye, er: epithelial roof, nm: neuromast. Stain with methylene blue/azure II/basic fuchsin.

Figure 7. Average weight (g) and length (cm) of meagre (*Argyrosomus regius*) reared in borehole (red) and natural seawater (blue). The values are mean±SD and asterisk indicate the statistically significant differences between the two water sources as indicated after independent t-test analysis ($p<0.05$).

Figure 8. Physicochemical parameters of the two water sources during the rearing trial with borehole water (red) and natural seawater (blue).

Figure 9. Meagre (*Argyrosomus regius*) reared in natural seawater (left) and borehole water (right) for 56 dph. All fish reared in borehole water had visible lesions on the head associated with CUD at the end of the rearing trial.

Figure 10. Cross sections of a supraorbital, an infraorbital and a mandibular canal of healthy (**A, C, E**) and CUD-affected meagre (*Argyrosomus regius*) (**B, D, F**). The canal roofs of the CUD-affected meagre showed hyperplasia and loss of the basal membrane while the neuromasts were exposed to the external environment. cr: canal roof, nm: neuromast. Stain with methylene blue/azure II/basic fuchsin.

Figure 11. μCT slices of healthy meagre's (*Argyrosomus regius*) head showing the cephalic canals from anterior (**A**) to posterior (**F**). Red asterisk: supraorbital canal, blue asterisk: infraorbital canal, green asterisk: mandibular canal.

Figure 12. μCT slices of CUD-affected meagre (*Argyrosomus regius*) head showing the cephalic canals from anterior (**A**) to posterior (**F**). The canal roofs of the affected fish were open with the neuromasts exposed to the external environment. Red asterisk: supraorbital canal, blue asterisk: infraorbital canal, green asterisk: mandibular canal.

Figure 13. SEM micrographs of healthy and CUD-affected juvenile meagre (*Argyrosomus regius*) (56 dph). Dorsal view showing the supraorbital canal (SO), the infraorbital canal (IO) and supraorbital commissure (SOCom) of healthy (**A**) and CUD-affected meagre (**B**). Lateral view of healthy (**C**) and CUD-affected meagre (**D**) showing the infraorbital canal, the nostril (R) and the mandibular canal (MD). Higher magnification of the nostril (N) with the supraorbital and the infraorbital canal (IO) of healthy (**E**) and CUD-affected meagre (**F**). Red arrows indicate the superficial neuromasts around the nostril.

Figure 14. SEM micrographs of CUD-affected meagre (*Argyrosomus regius* – 56 dph). **A**: Lateral view of the head with the ulcerative nostril, supraorbital (red arrow) and infraorbital canal (green frame). The olfactory rosette was not affected. **B**: Higher magnification of the nostril with the opened infraorbital canal (red arrow). Framed area indicates normal superficial neuromasts around the nostril. **C-D**: Higher magnification of the superficial neuromasts around the nostril. **E**: Higher magnification of the infraorbital canal with the exposed canal neuromast. **F**: Higher magnification of the exposed canal neuromast showing the normal sensory hair cells. **G:** Dorsal view of the opened supraorbital canal with the exposed neuromasts (red arrows, red frame). **H**: Higher magnification of the exposed neuromast from the framed area of picture G.

Figure 15. Nine-month-old meagre (*Argyrosomus regius*) reared **A:** exclusively in borehole seawater **B:** in borehole water for 4 months and transferred to natural seawater for 5 months, with partial resolution of the lesions. **C:** in borehole water for 4 months and transferred to natural seawater for 5 months, with complete resolution of the lesions

Figure 16. Relative expression of CathK, TRAP and vATPase in heads of healthy and CUD-affected meagre (*Argyrosomus regius*) at the end of the rearing trial (56 dph). Values are means+SD while (*) indicates statistically significant differences between the two groups ($p < 0.05$).

Figure 17. Relative expression of Hsp70, Hsp90, phospho p38 MAPK και phospho p44/42 MAPK in heads of healthy and CUD-affected meagre (*Argyrosomus regius*) at the end of the rearing trial (56 dph). Values are means+SD while asterisk (*) indicates statistically significant differences between the two groups ($p < 0.05$).

Figure 18. Physicochemical parameters of the two water sources during the rearing trial with natural seawater (blue) and natural seawater+CO_2 (red).

Figure 19. Meagre (*Argyrosomus regius*) reared in natural seawater (left) and natural seawater+CO_2 (right) at the end of the rearing trial (60dph). None of the fish reared in natural seawater+CO_2 had visible lesions associated with CUD.

Figure 20. Cross sections of the fully formed lateral line canals on the head of meagre (*Argyrosomus regius*) reared in natural seawater+CO_2 (60 dph, TL: 5,65 ± 0,49 cm). **A:** Supraorbital canal (magnification: x1). **B:** Mandibular canal (magnification: x3). **C:** Infraorbital canal (magnification: x3). No lesions associated with CUD were observed in any of the canals. b: brain, cr: canal roof, e: eye. Stain with methylene blue/azure II/basic fuchsin.

767

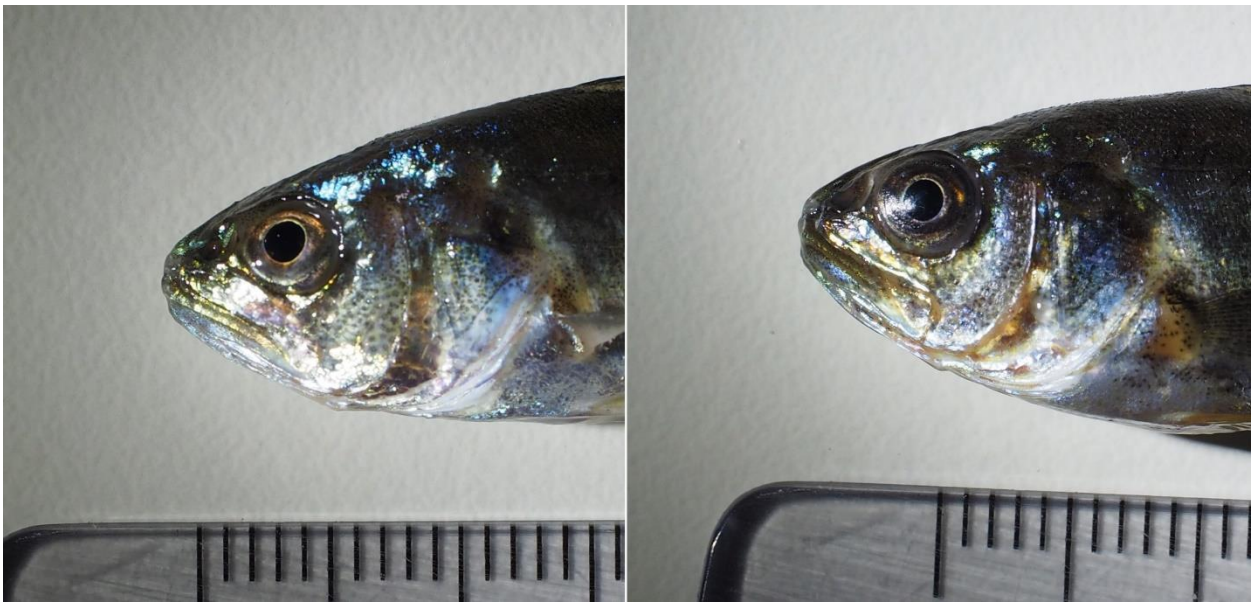

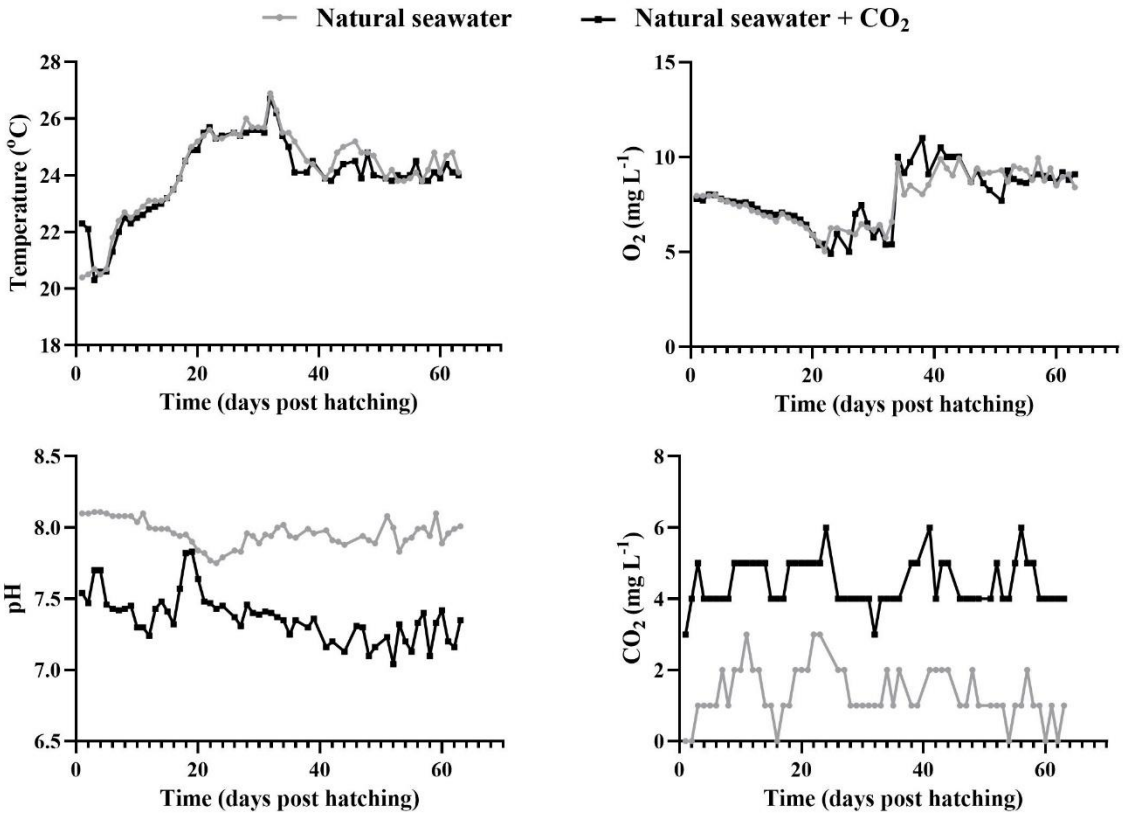
Natural seawater
Natural seawater + CO_2
Temperature (°C)
O_2 (mg L^{-1})
pH
CO_2 (mg L^{-1})
Time (days post hatching)

768

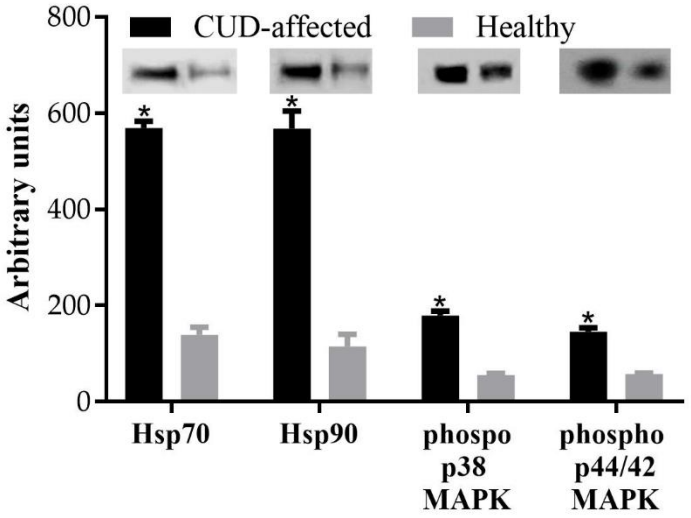
800
600
400
200
0
Arbitrary units
CUD-affected
Healthy
*
*
*
*
Hsp70
Hsp90
phospo p38 MAPK
phospho p44/42 MAPK

769

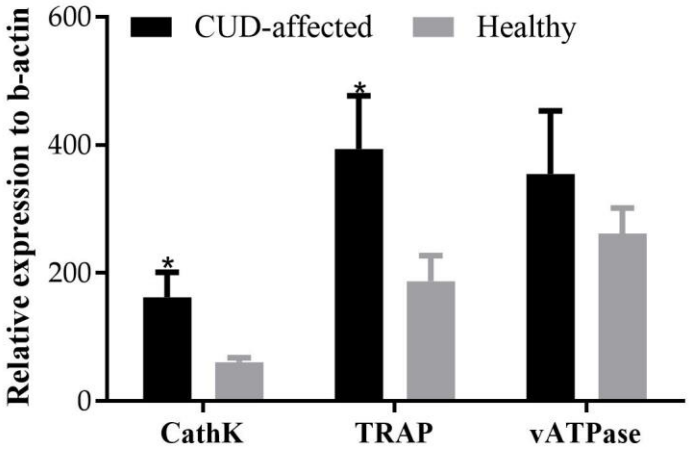
600
400
200
0
Relative expression to b-actin
CUD-affected
Healthy
*
*
CathK
TRAP
vATPase

770

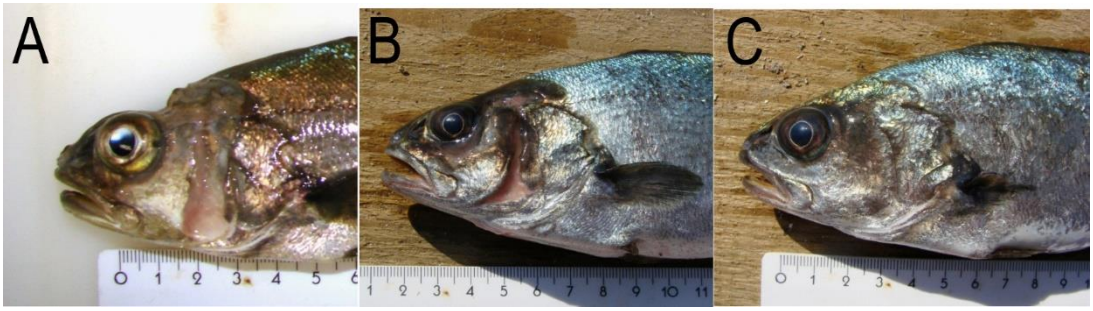
A
B
C

771

772

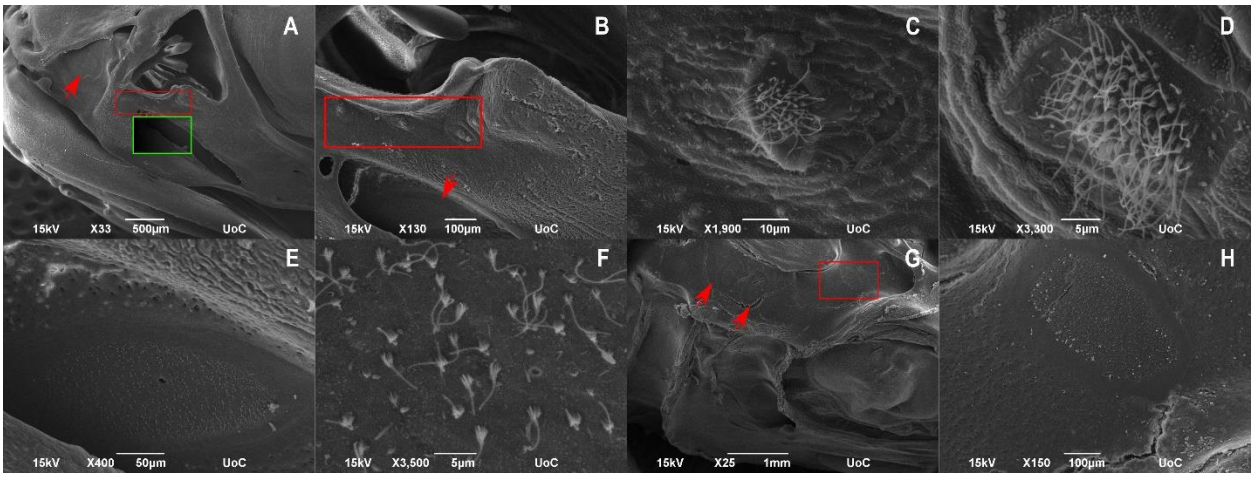
A
15kV X33 500µm UoC
B
15kV X130 100µm UoC
C
15kV X1,900 10µm UoC
D
15kV X3,300 5µm UoC
E
15kV X400 50µm UoC
F
15kV X3,500 5µm UoC
G
15kV X25 1mm UoC
H
15kV X150 100µm UoC

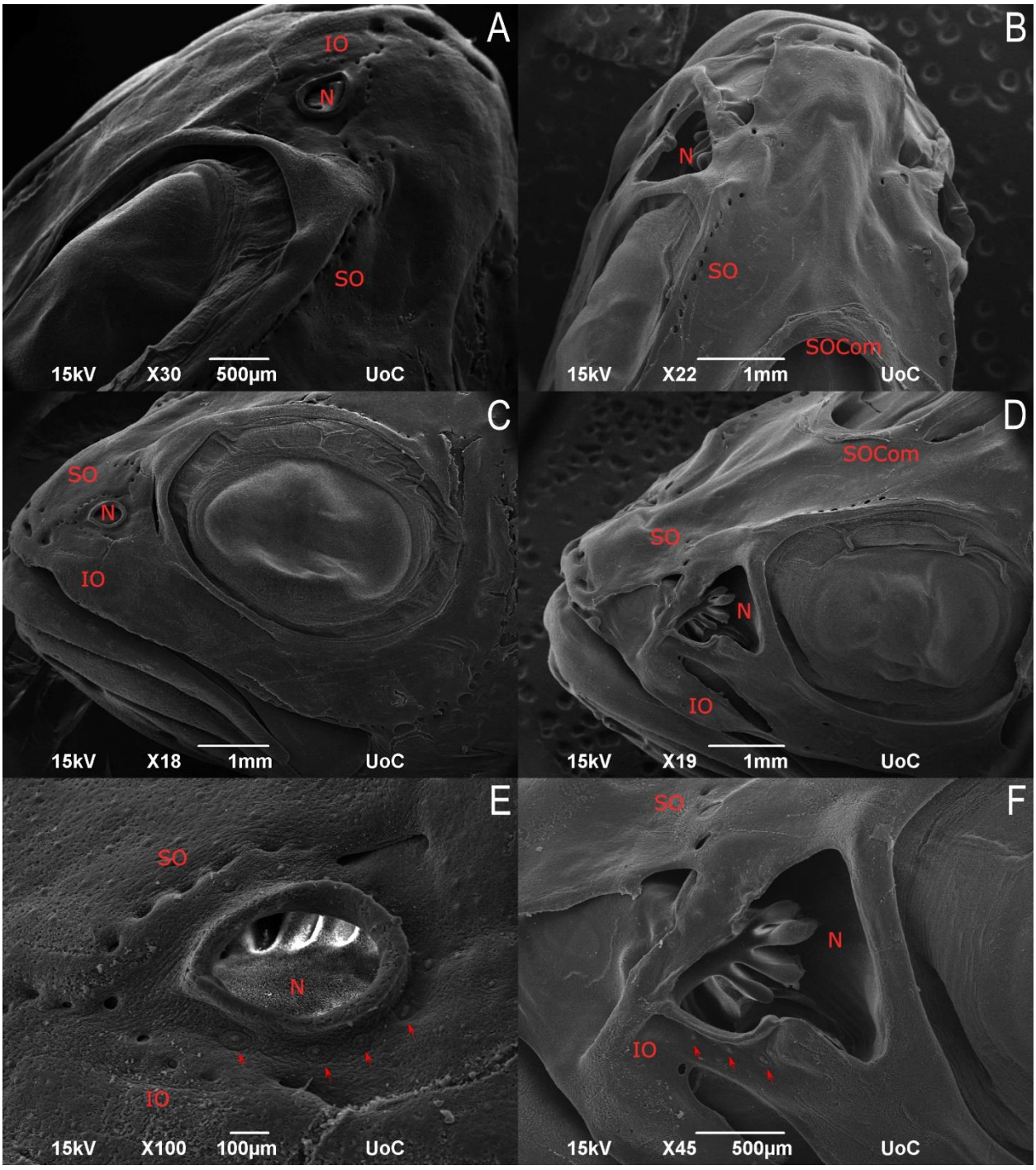
A
IO
N
SO
15kV X30 500µm UoC
B
N
SO
SOCom
15kV X22 1mm UoC
C
SO
N
IO
15kV X18 1mm UoC
D
SOCom
SO
N
IO
15kV X19 1mm UoC
E
SO
N
IO
15kV X100 100µm UoC
F
SO
N
IO
15kV X45 500µm UoC

773

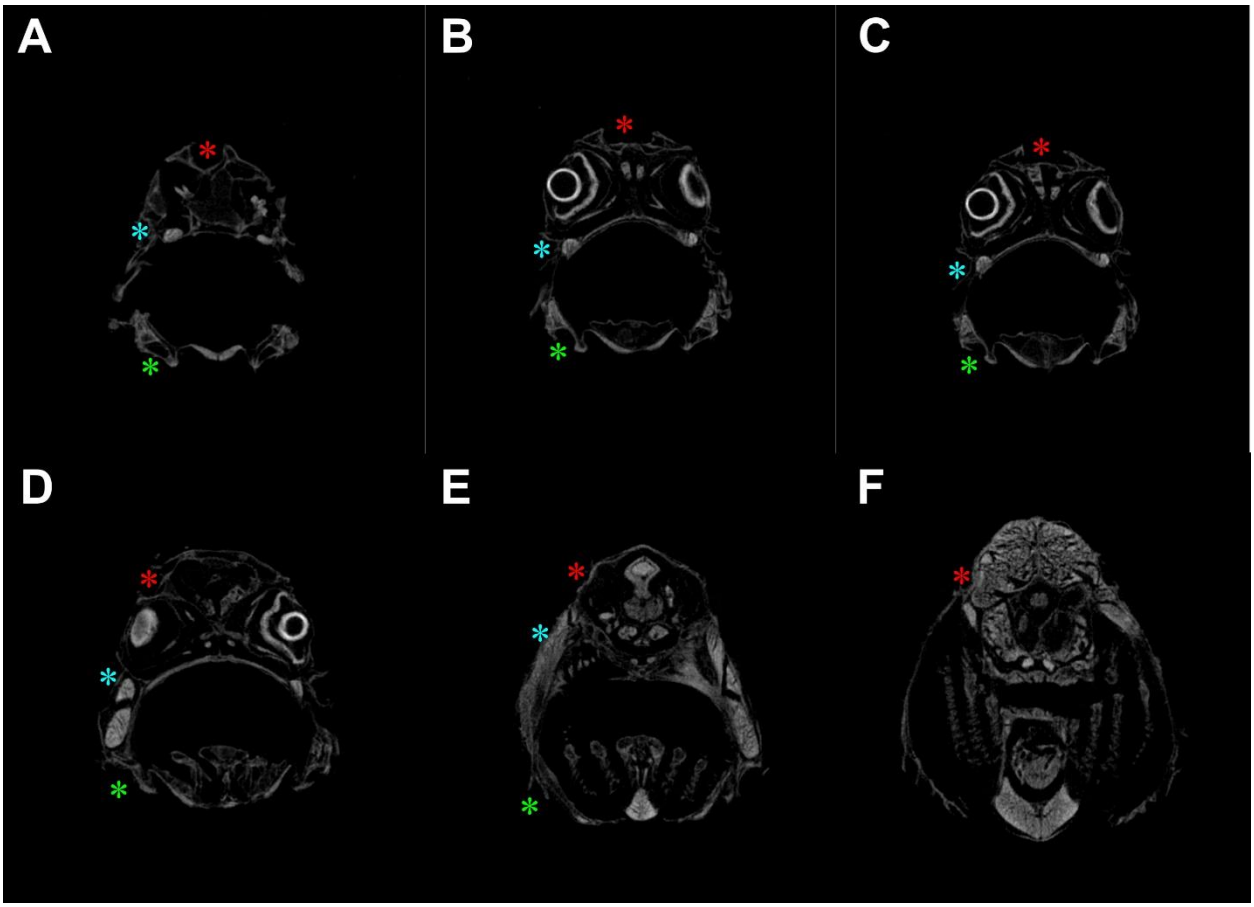

774

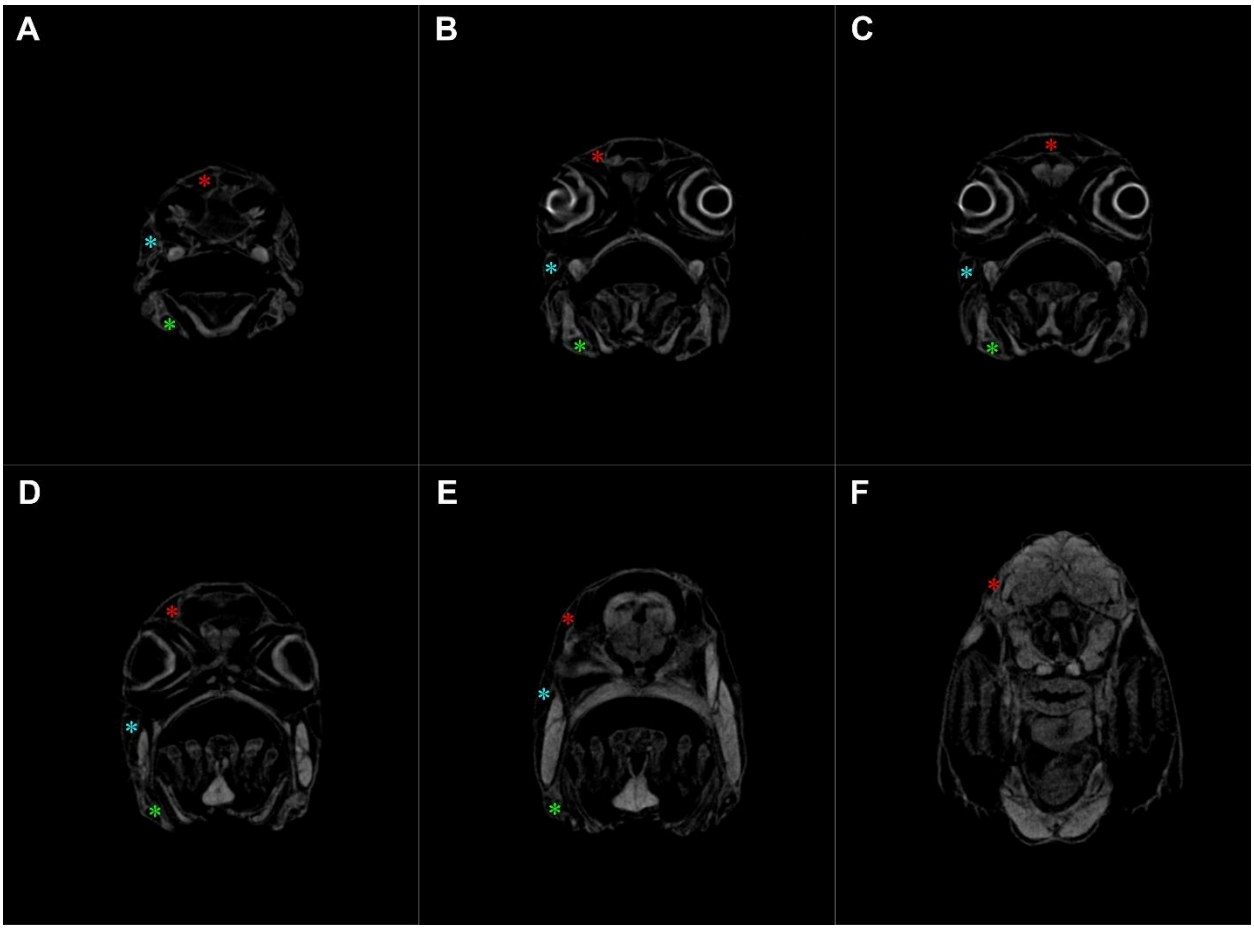

775

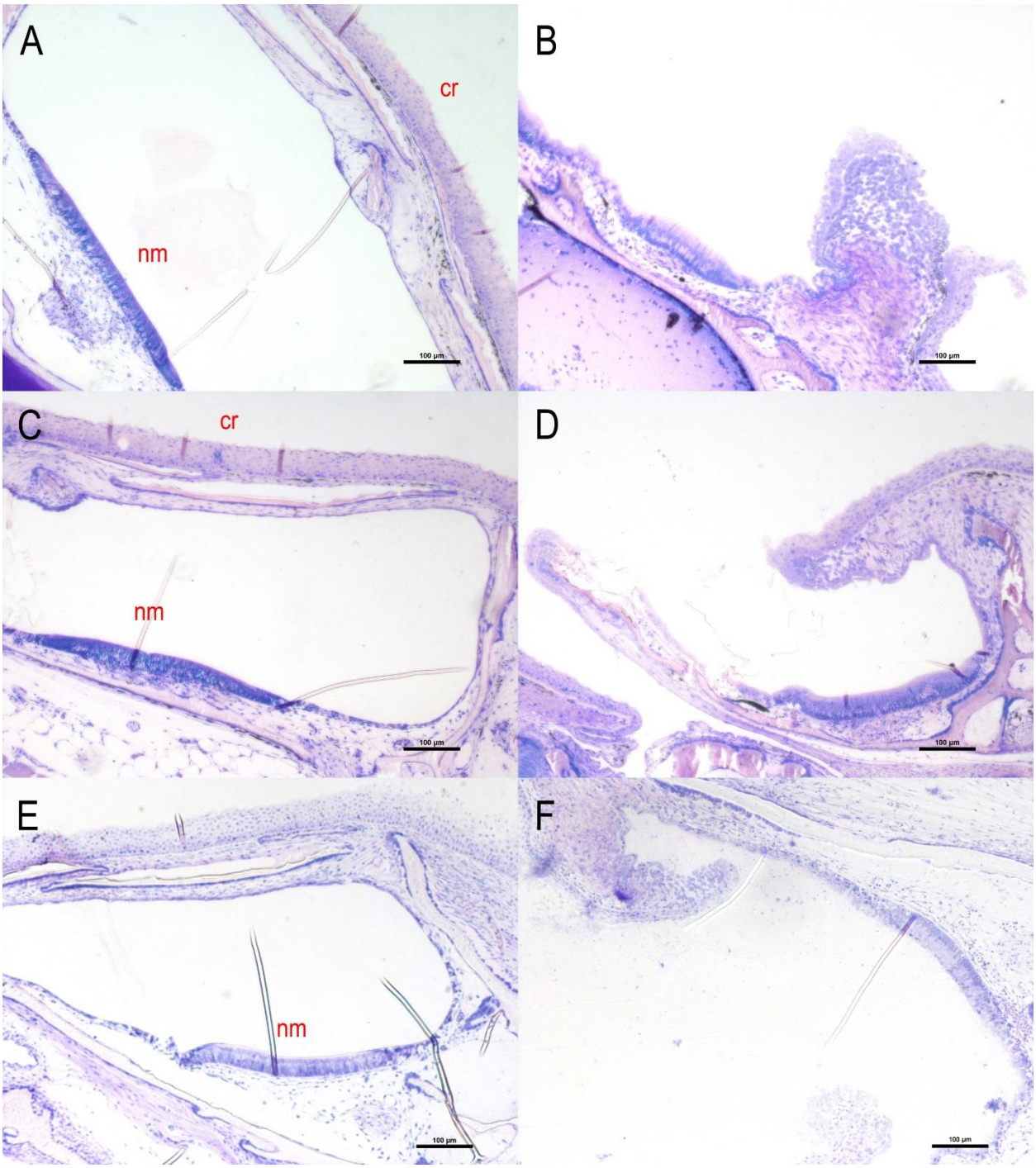

776

777

778

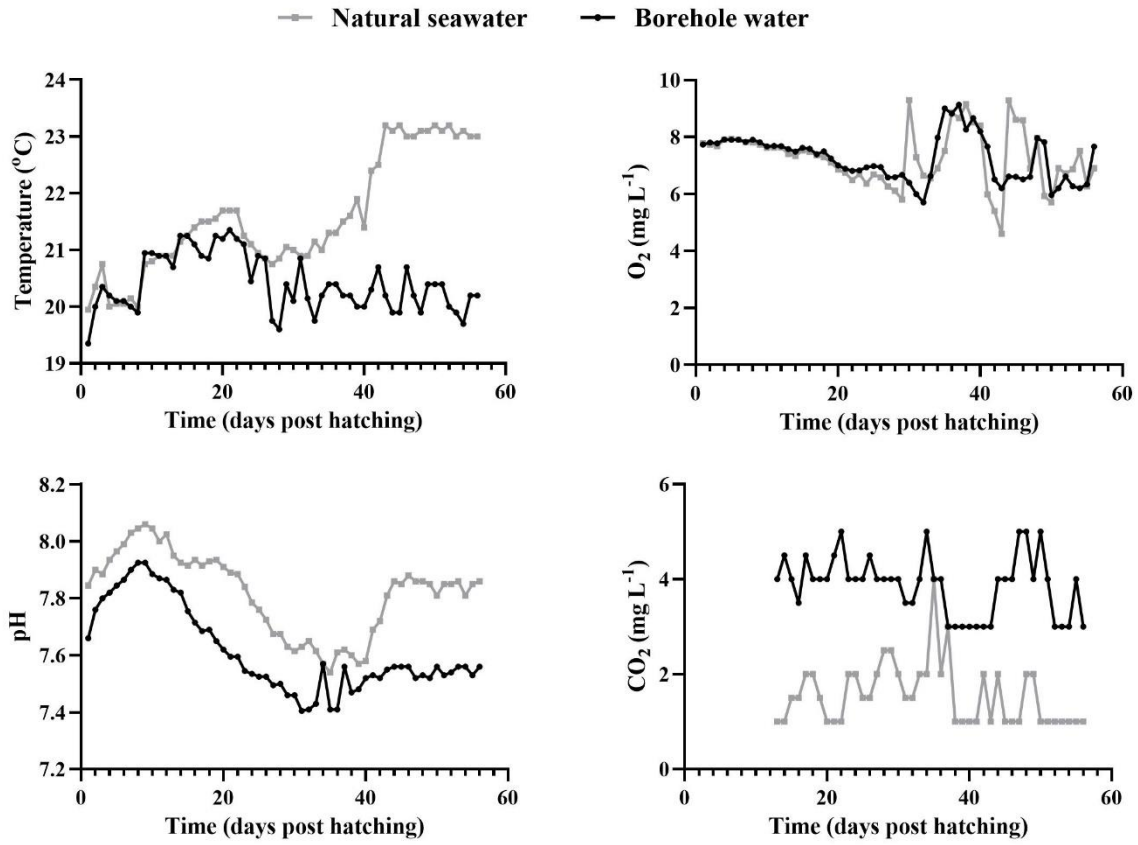
Natural seawater
Borehole water
Temperature (°C)
Time (days post hatching)
O_2 (mg L^{-1})
Time (days post hatching)
pH
Time (days post hatching)
CO_2 (mg L^{-1})
Time (days post hatching)

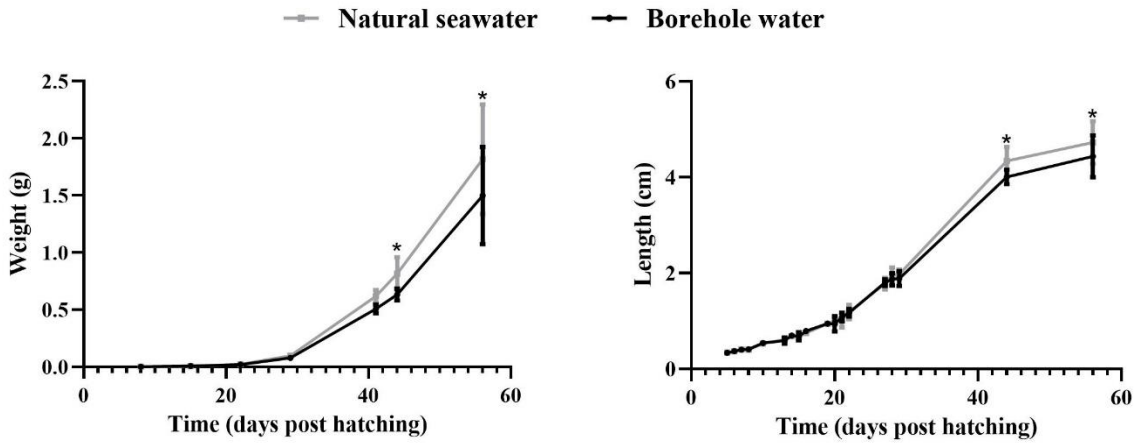
Natural seawater
Borehole water
Weight (g)
Time (days post hatching)
Length (cm)
Time (days post hatching)

779

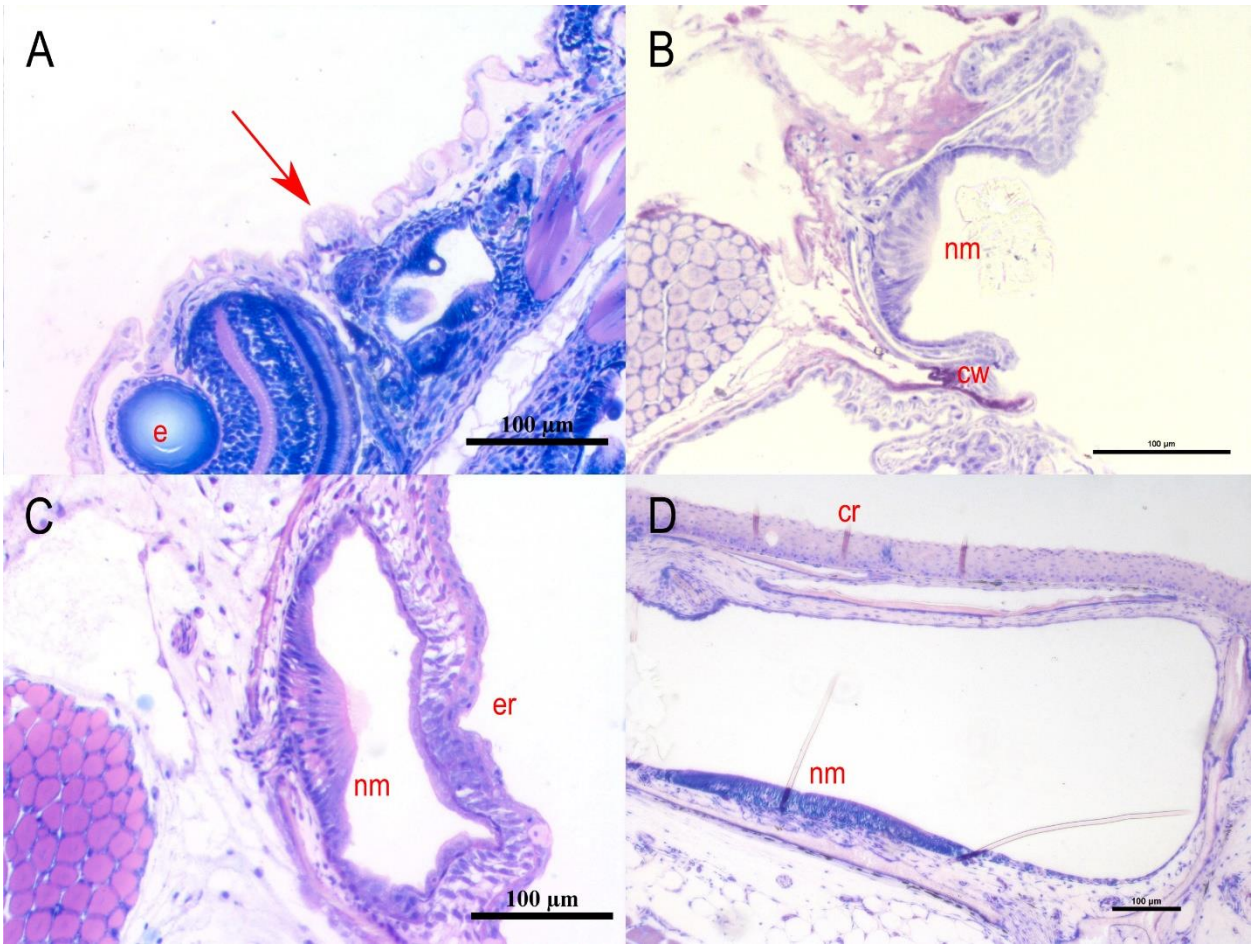
A
e
100 µm
B
nm
cw
C
er
nm
100 µm
D
cr
nm

780

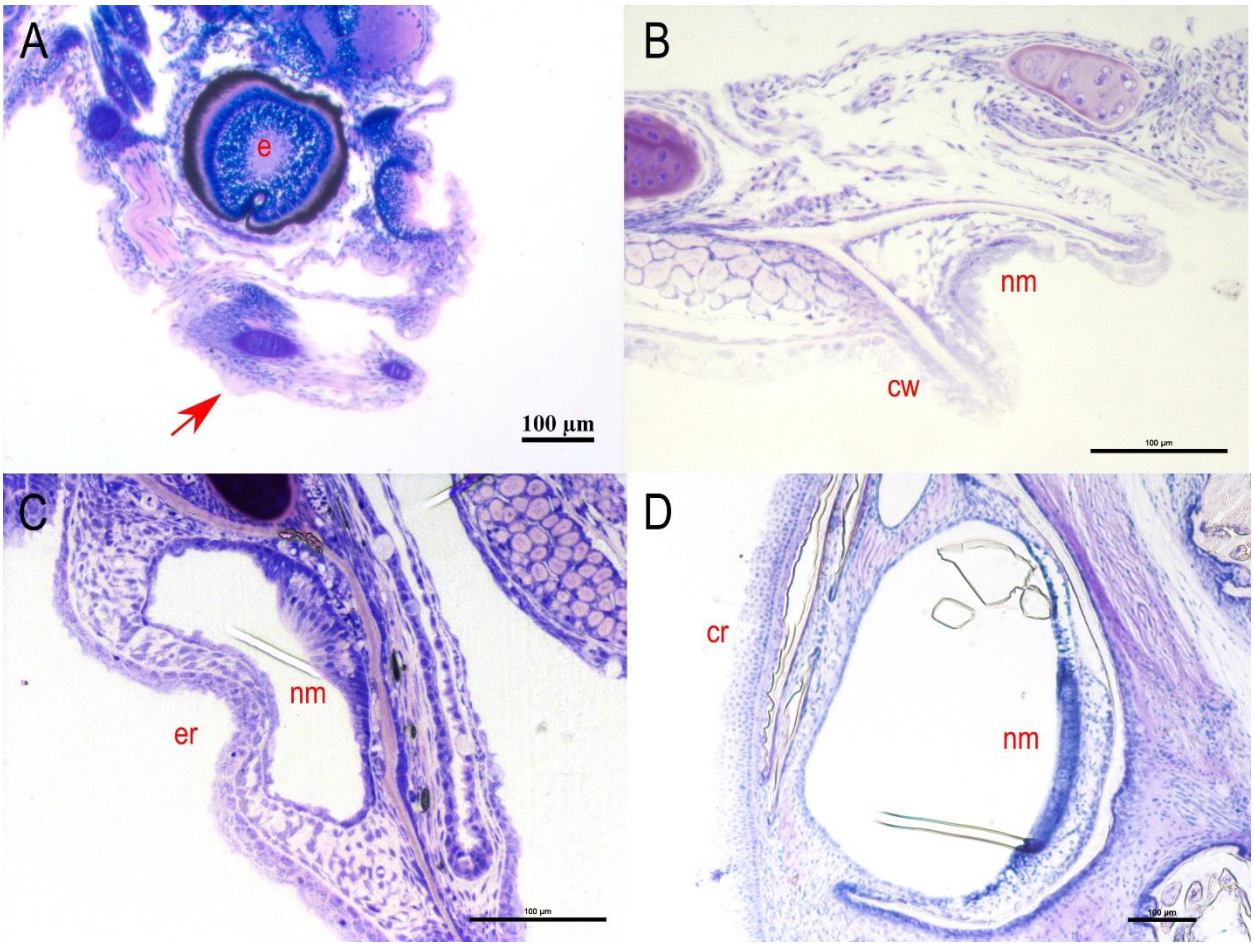

781

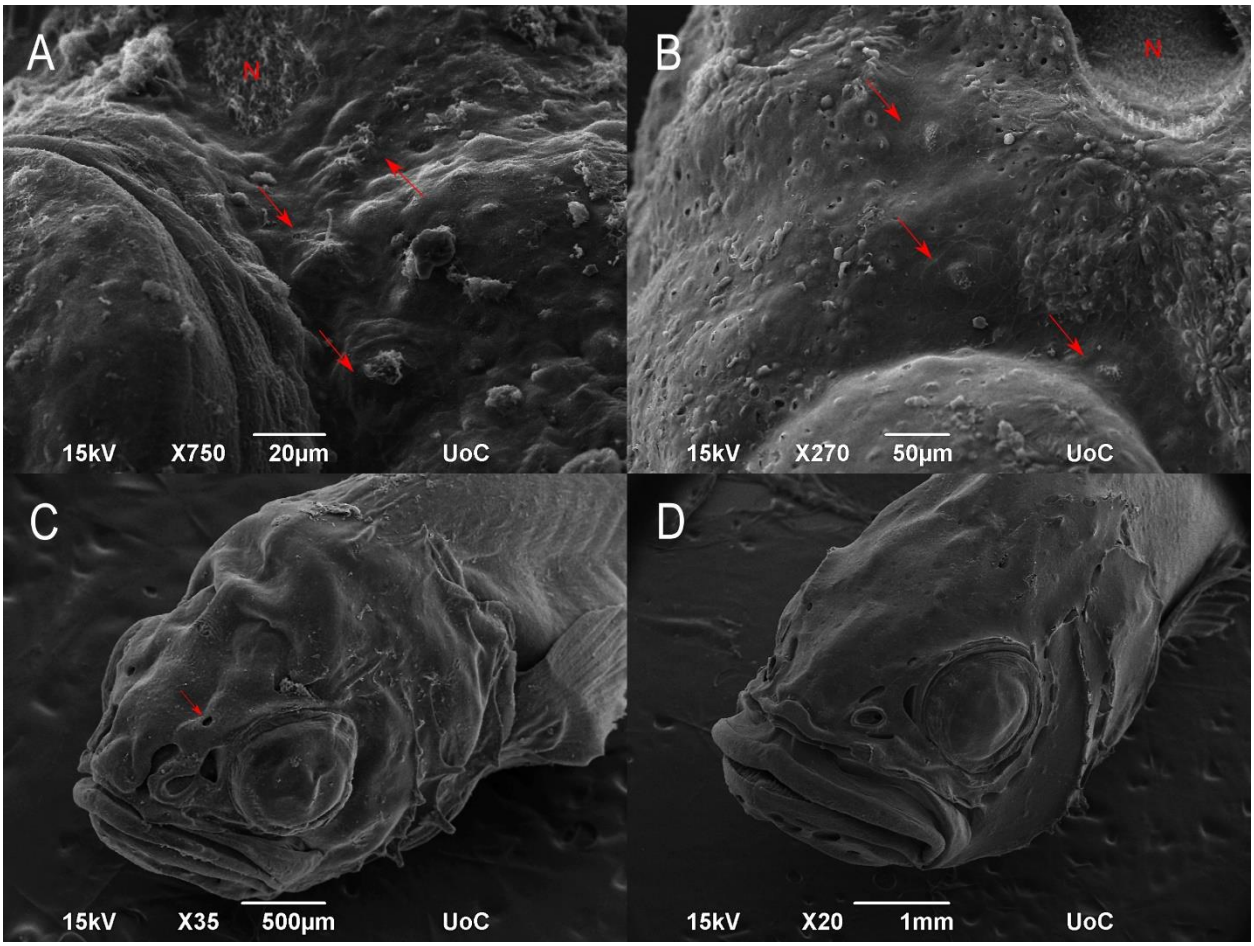
A
N
15kV X750 20µm UoC
B
N
15kV X270 50µm UoC
C
15kV X35 500µm UoC
D
15kV X20 1mm UoC

782

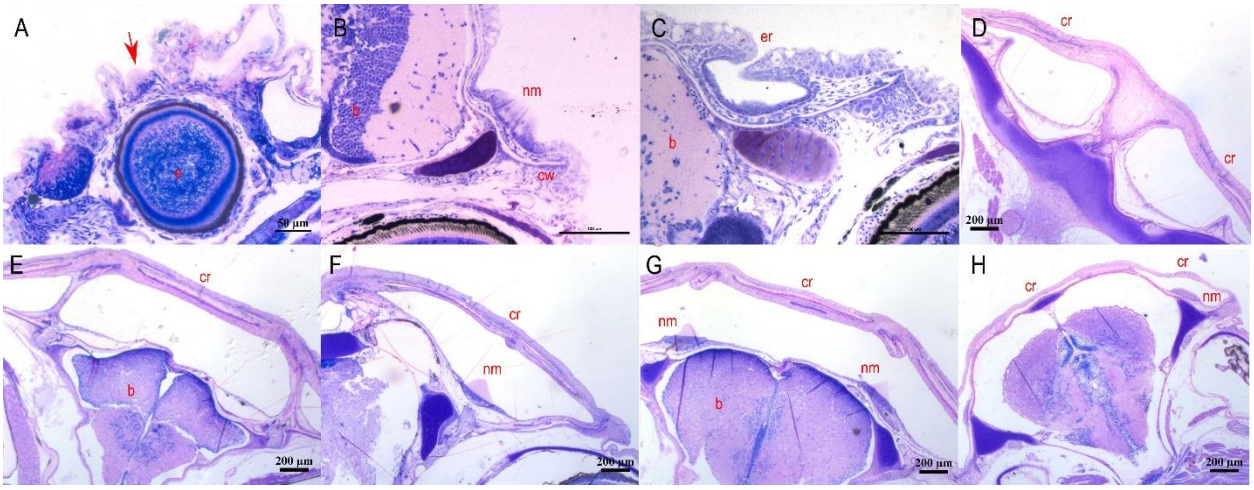
A
B
nm
cw
C
er
b
D
cr
E
cr
b
F
cr
nm
G
cr
nm
nm
b
H
cr
cr
nm

783

784

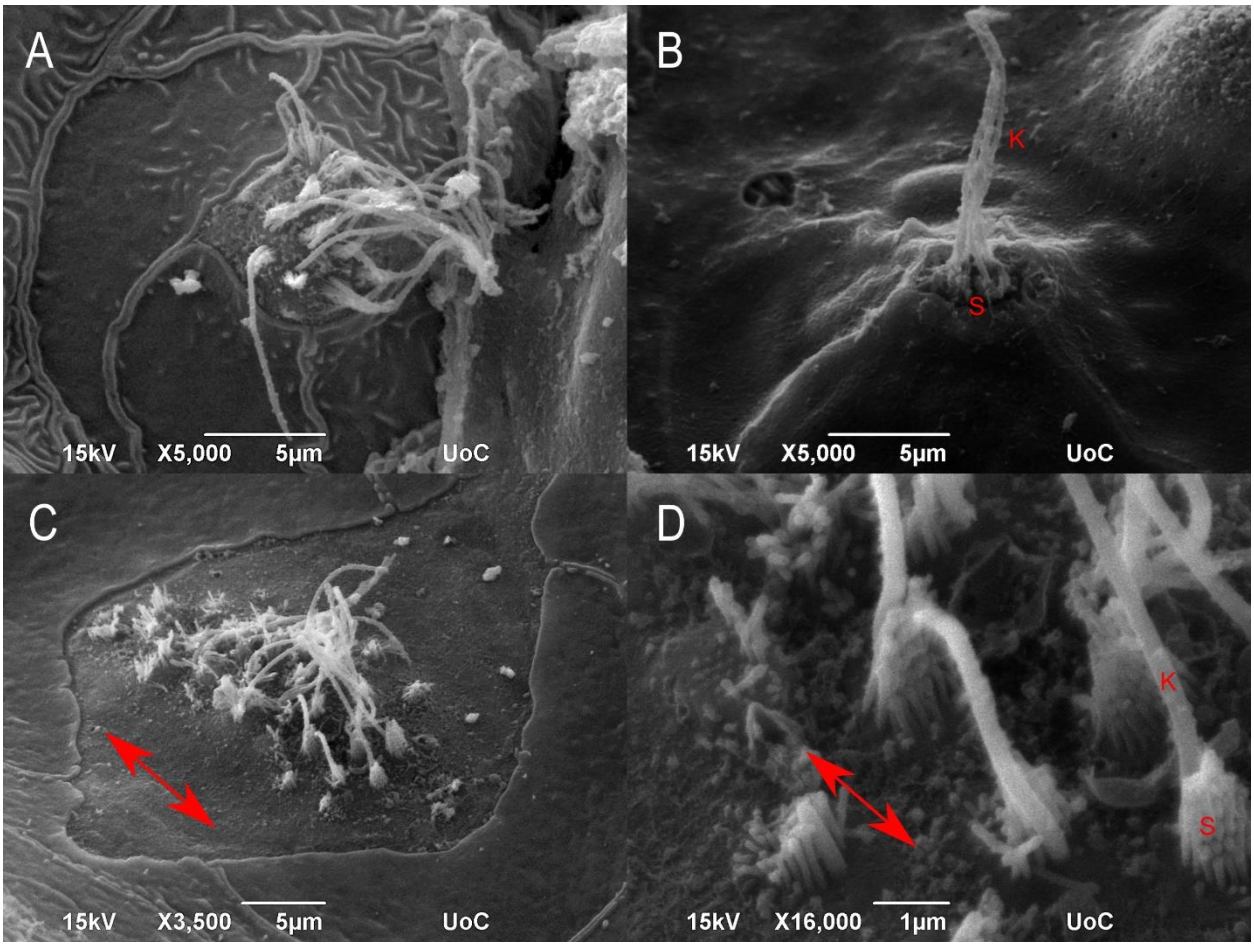
A
15kV X5,000 5µm UoC
B
K
S
15kV X5,000 5µm UoC
C
15kV X3,500 5µm UoC
D
K
S
15kV X16,000 1µm UoC

785

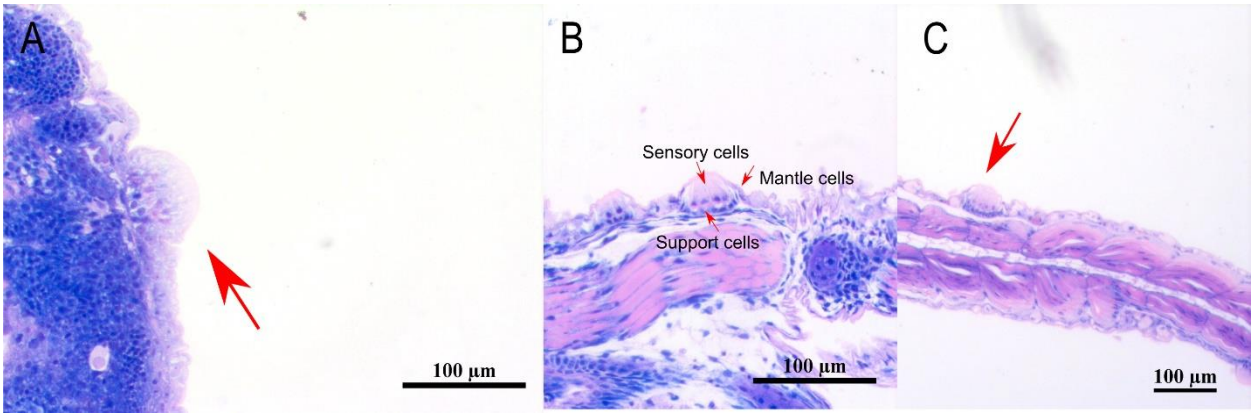
A
100 µm
B
Sensory cells
Mantle cells
Support cells
100 µm
C
100 µm

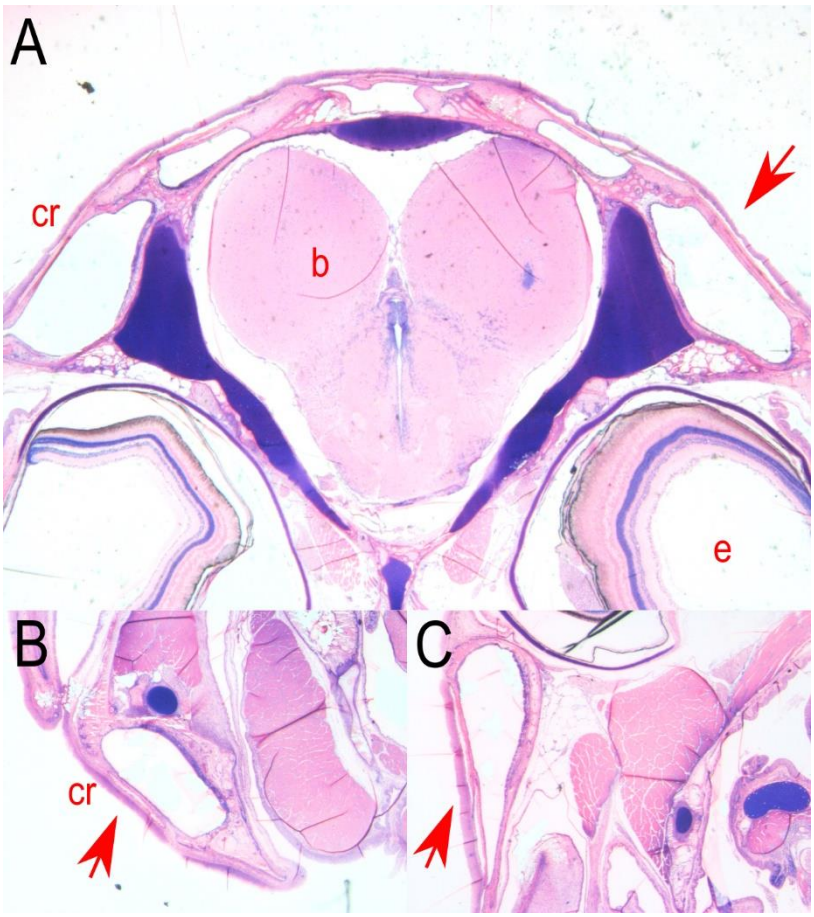

786